Potential Laramide/Oceanic Plateau Topics

1. The track of the oceanic plateau (“Shatsky Rise Conjugate”) is sufficiently well established that meaningful tests can be made. [Basically, if we don’t know where it was and instead are using the geologic changes in North America to plot its course, those geologic features cease to be useful as a test of the hypothesis; we then have to distinguish the features used to set the track from whatever is left that might test the idea].
2. Subduction of an oceanic plateau will cause surface uplift in the continent. [This is a subset of the models out there] **- Elize, (Shunjie)**
3. Subduction of an oceanic plateau will lead to subsidence in the continental interior [Also a subset of models]**-Shunjie**
4. Subduction of an oceanic plateau will usher in flat slab subduction
5. Subduction of the Shatsky Conjugate produced the Rand+/-Orocopia+/-Pelona schists in the Mojave Desert
6. Timing of vertical changes in surface elevation (see points 2 and 3) is in agreement with geological proxies such as changes in fluvial systems, major unconformities, etc.**-Vanessa**
7. The stress field induced by the Shatsky Conjugate is consistent with coeval deformation in North America**-Stephen**
8. Subduction of the Shatsky Conjugate has left fragments in coastal accretionary complexes
9. Magmatism patterns are consistent with the history of subduction of the Shatsky Conjugate.**-Keely, (Stephen), Tyler**
10. Timing of deformation in the Laramide is consistent with the passage of the Shatsky Conjugate.

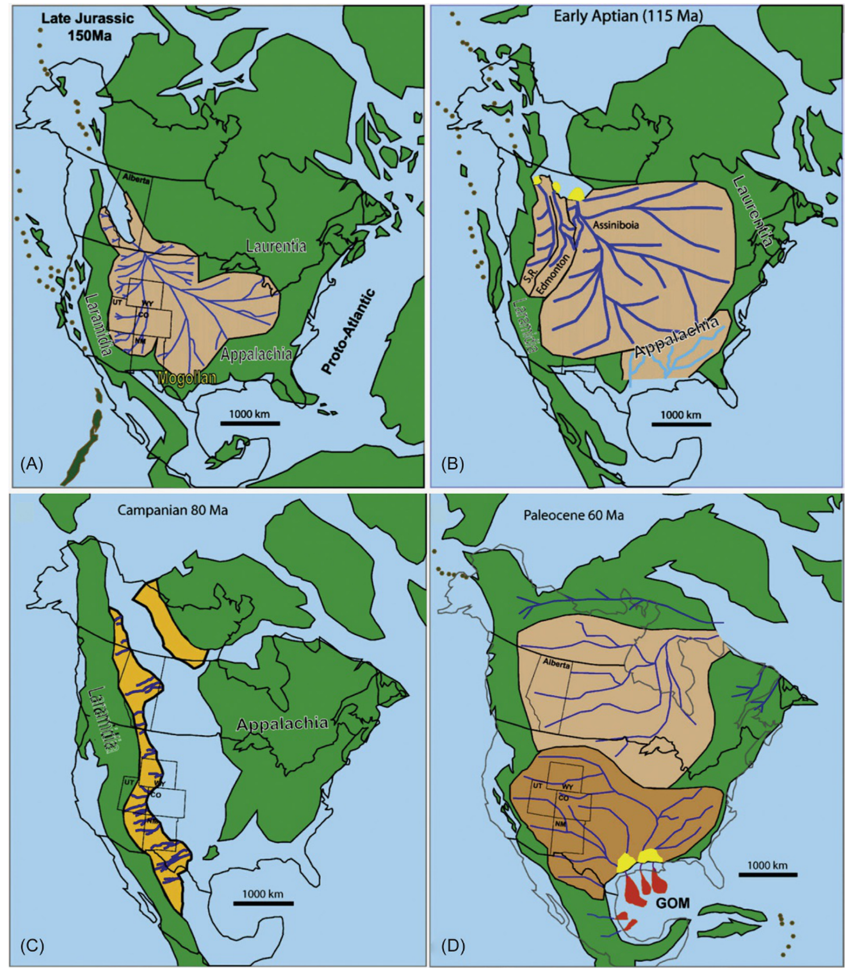

Maill & Catuneanu, in *Sed Basins US & Canada*, 2019

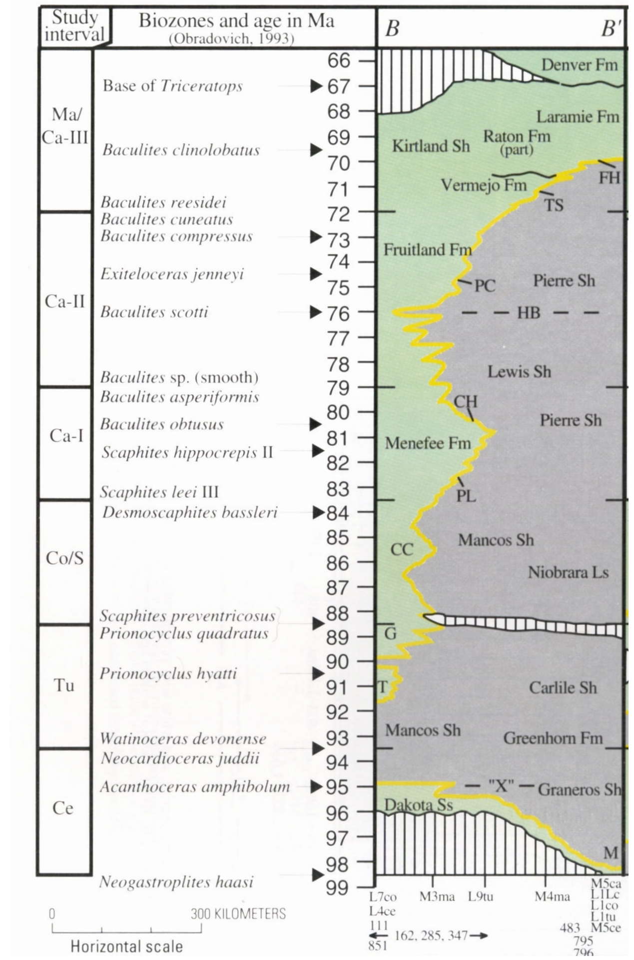

Roberts and Kirschbaum, USGS PP 1561

Durango

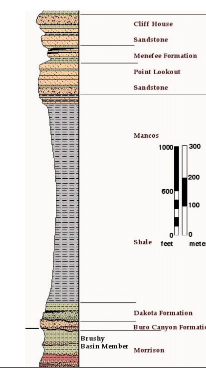

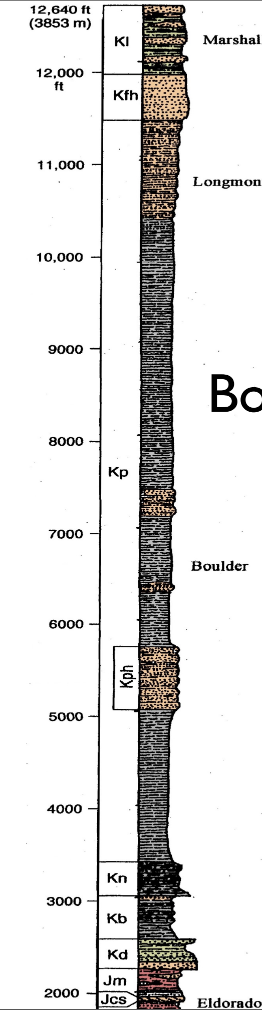

Boulder

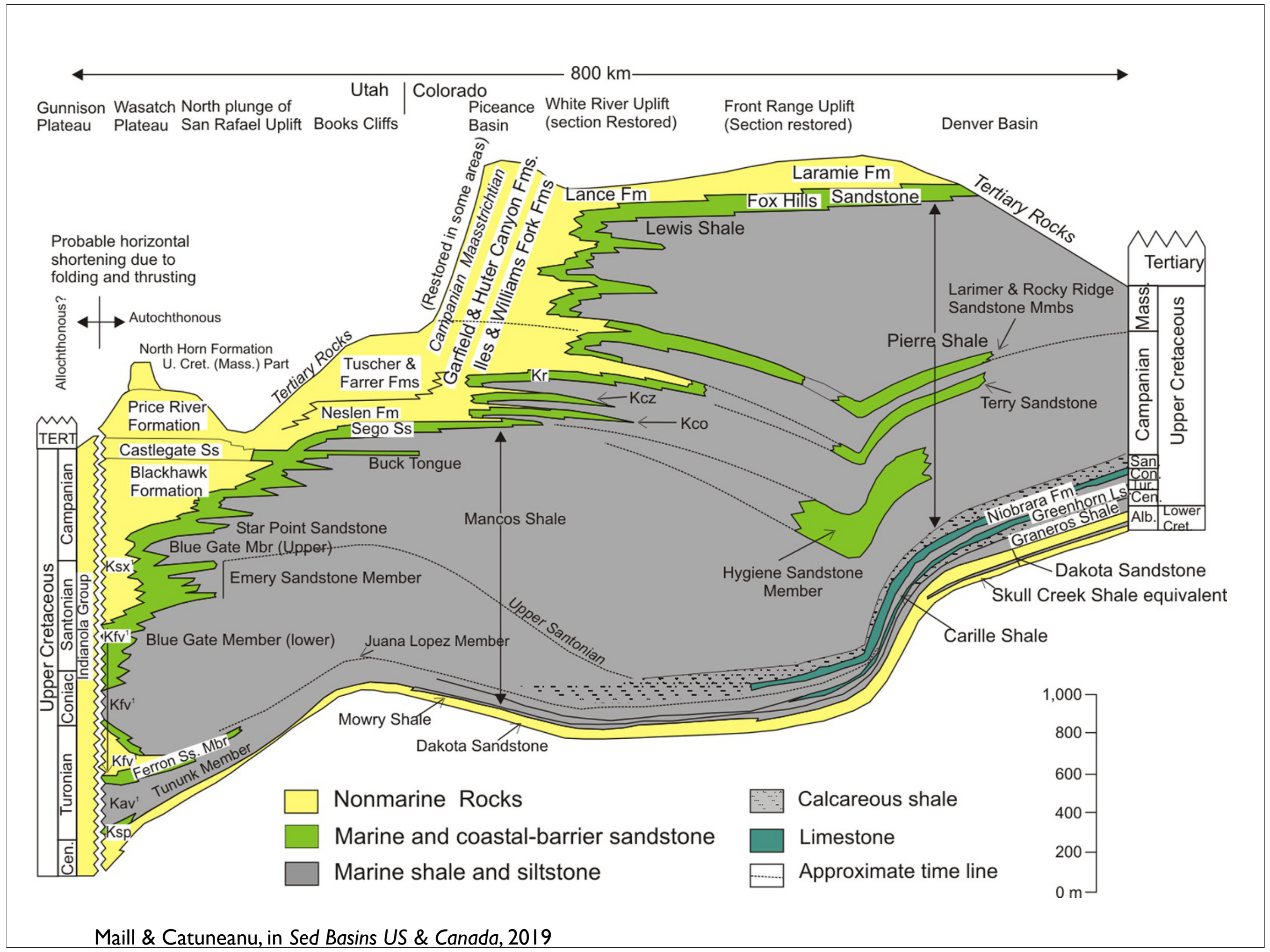

FIG. 7 Stratigraphic cross-section of Cretaceous rocks from central Utah to northeastern Colorado. Thicknesses are based on well and outcrop control. Vertical exaggeration approximately ×151. The Castlegate Sandstone has been interpreted as a product of “antitectonic” sedimentation (Yoshida et al., 1996). Colors were utilized in the paleogeographic maps. Abbreviations: Ksx, Sixmile Canyon Formation; Kfv, Funk Valley Formation; Kav, Allen Valley Formation; Ksp, Sanpete Formation; Kr, Rollins Sandstone Member; Kcz, Cozzette Sandstone Member; Kco, Corcoran Sandstone Member. (From Molenaar and Rice (1988).)

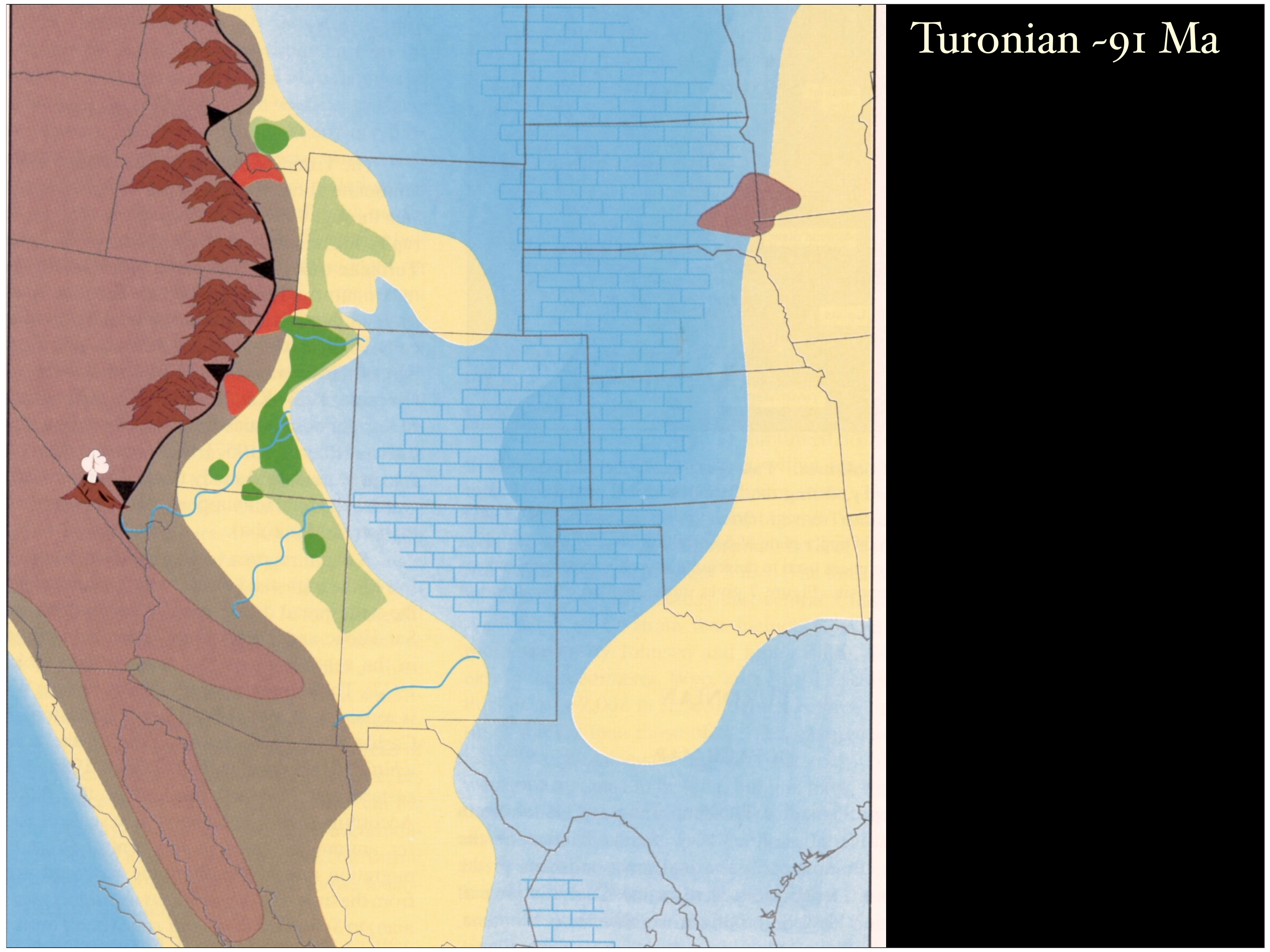

Explain what the colors are (greens are areas accumulating coals, bricks are carbonates). One initial question is, why a seaway? Classically, this was thought to largely be high stand of ocean

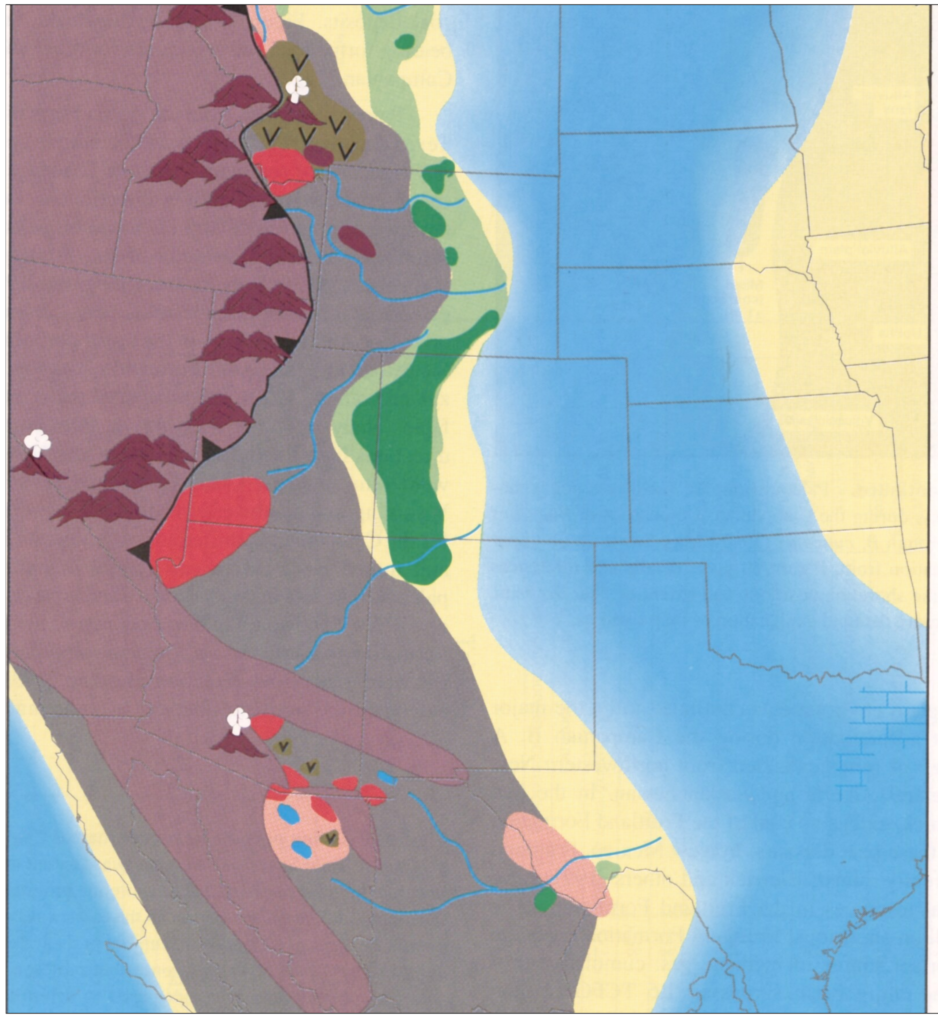

Campanian
~75 Ma

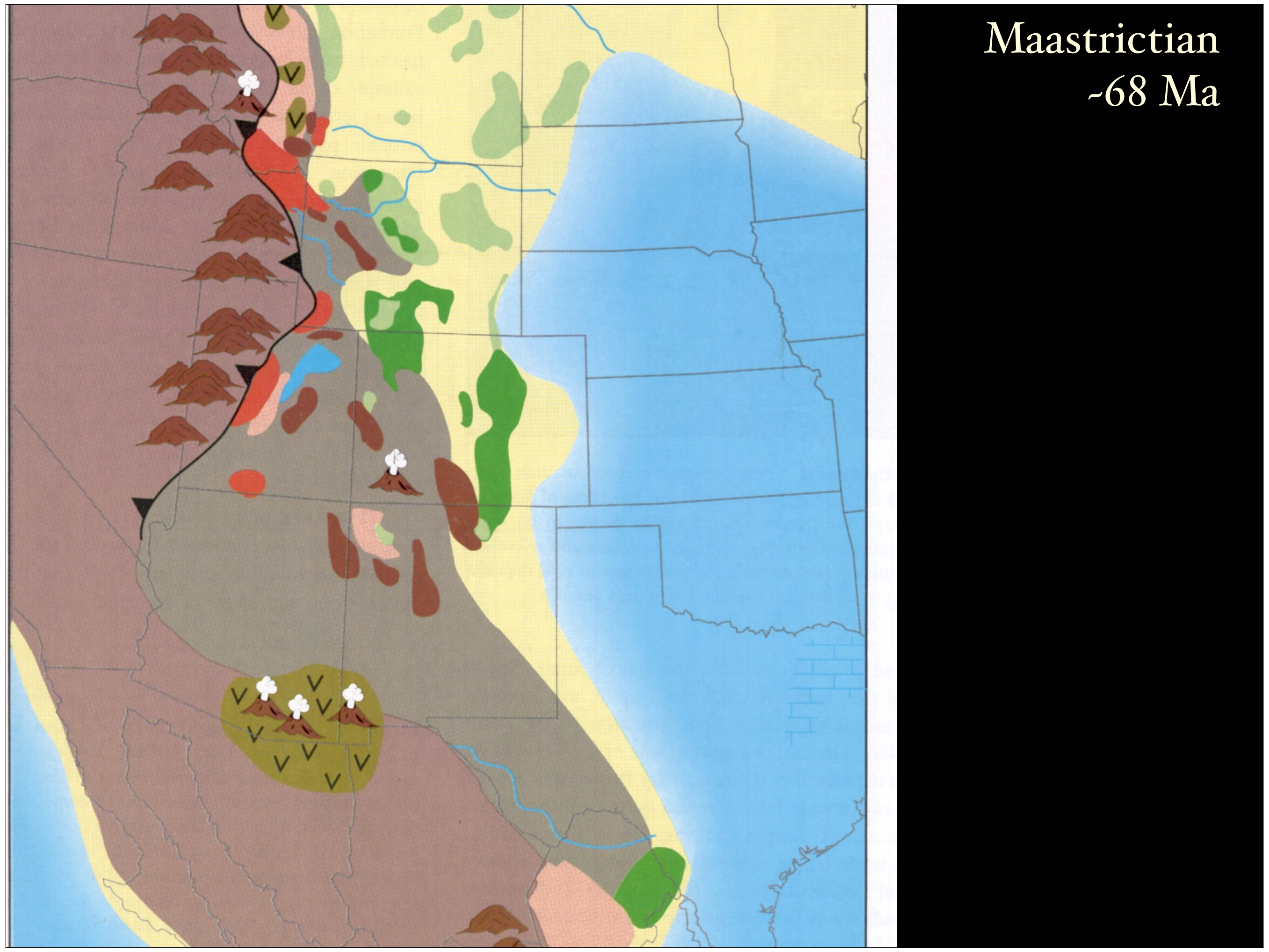

Seems like an orderly progradation of terrestrial facies out into the seaway…but look at sediment accumulation…

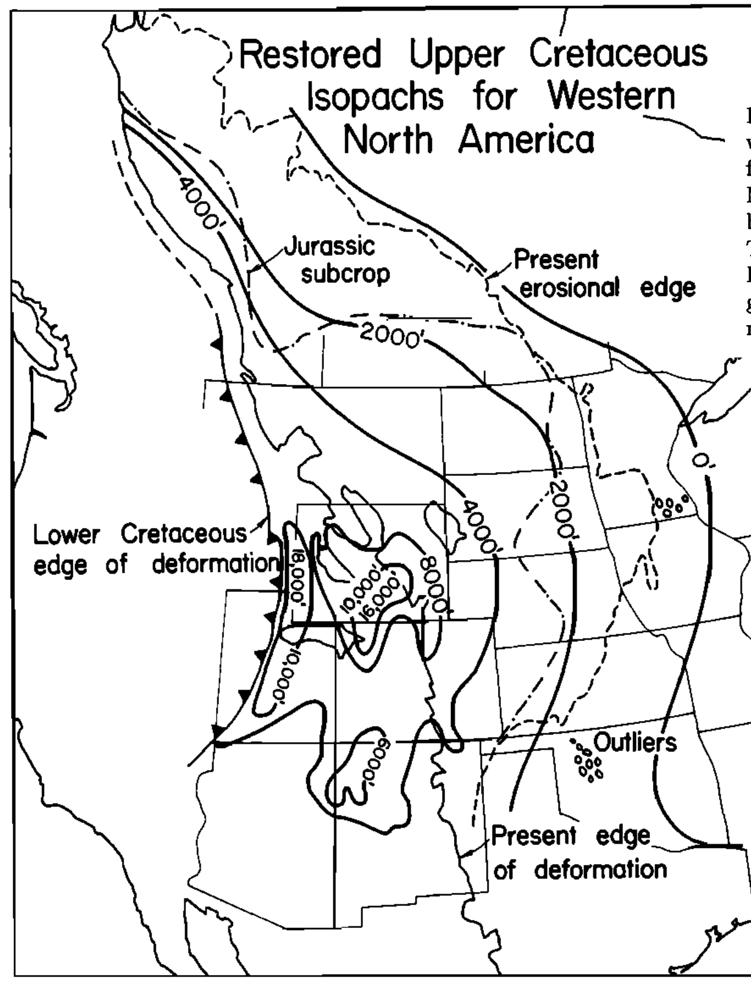

Fig. 1. Restored Upper Cretaceous isopach map for western North America. Data for the United States are from Cross and Pilger [1978b]. Data for Canada are from McCrossan and Glaister [1966]. Contours are given in feet because the original data are presented in this manner. The irregular pattern in Wyoming and Colorado is due to Laramide tilted block movements in the foreland. It is the general pattern and great width of the sedimentation that requires explanation.

Mitrovica et al., Tectonics, 1989

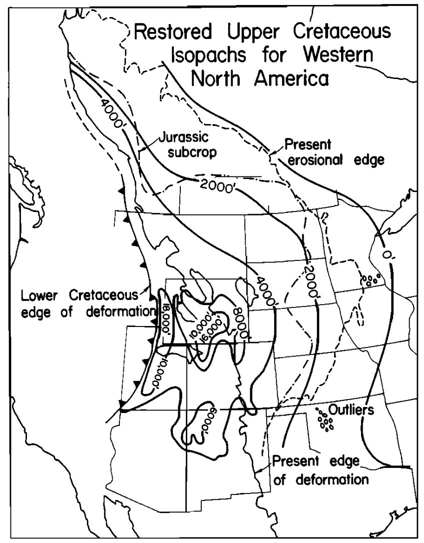

Fig. 1. Restored Upper Cretaceous isopach map for western North America. Data for the United States are from Cross and Pilger [1978b]. Data for Canada are from McCrossan and Glaister [1966]. Contours are given in feet because the original data are presented in this manner. The irregular pattern in Wyoming and Colorado is due to Laramide tilted block movements in the foreland. It is the general pattern and great width of the sedimentation that requires explanation.

Mitrovica et al., Tectonics, 1989

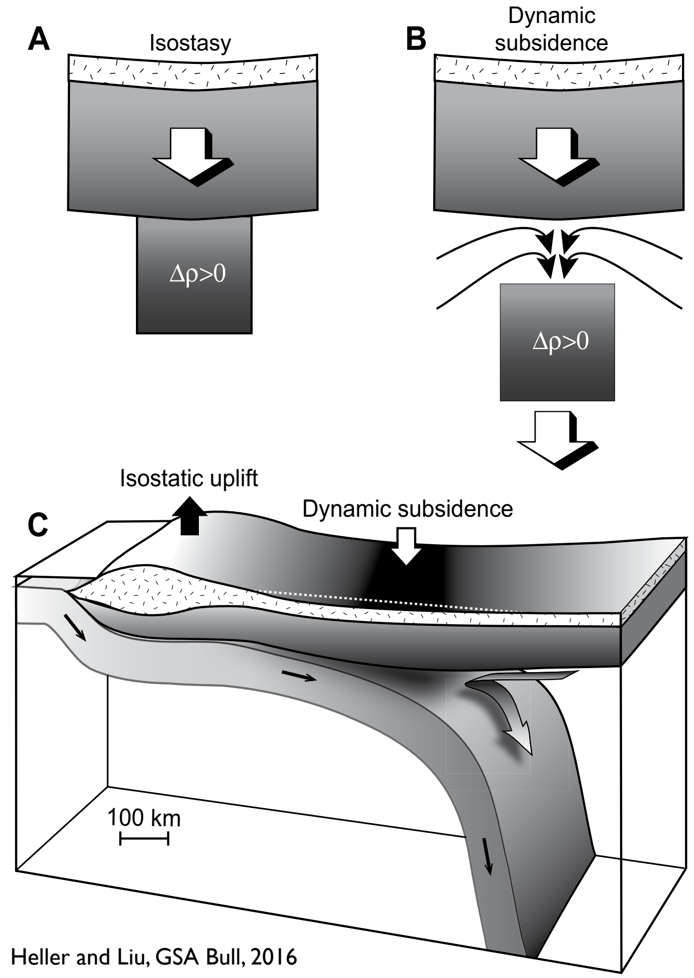

Heller and Liu, GSA Bull, 2016

We need something to pull crust down at least in some areas. What exactly can do this–what is “dynamic subsidence”

Viscous fluids

In a Newtonian fluid, if horizontal velocity is u and vertical is v, then the shear stress in the fluid is related to the gradient in velocity:

$$\tau_{zx} = \eta \frac{du}{dz}$$

Applying continuity (conservation of fluid) and assuming equilibrium, can be shown that the dynamic pressure P is related to variations in fluid velocity u and v (horizontal and vertical):

$$\frac{\partial P}{\partial x} = \eta\left(\frac{\partial^2 u}{\partial x^2} + \frac{\partial^2 u}{\partial z^2}\right)$$

$$\frac{\partial P}{\partial z} = \rho g + \eta\left(\frac{\partial^2 v}{\partial x^2} + \frac{\partial^2 v}{\partial z^2}\right)$$

$$P_{slabtop} = \frac{-8.558\eta U}{r} \text{ for dip=45°}$$

$$P_{slabbottom} = \frac{+0.462\eta U}{r} \text{ for dip=45°}$$

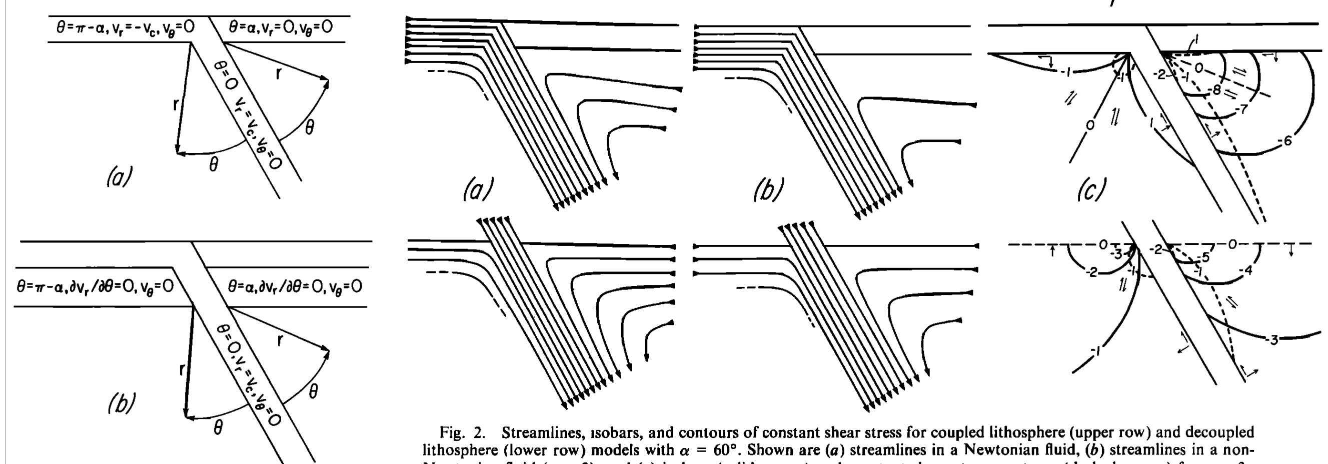

ner flow models for (*a*) coupled lithosphere and (*b*) decoupled iosphere.

Fig. 2. Streamlines, isobars, and contours of constant shear stress for coupled lithosphere (upper row) and decoupled lithosphere (lower row) models with α = 60°. Shown are (*a*) streamlines in a Newtonian fluid, (*b*) streamlines in a non-Newtonian fluid (n = 3), and (*c*) isobars (solid curves) and constant shear stress contours (dashed curves) for n = 3.

Tovish et al., JGR, 1978

Math from Turcotte and Schubert section 6.11. Torque is force x distance, so torque from tip of asthenospheric counterflow is constant downslab

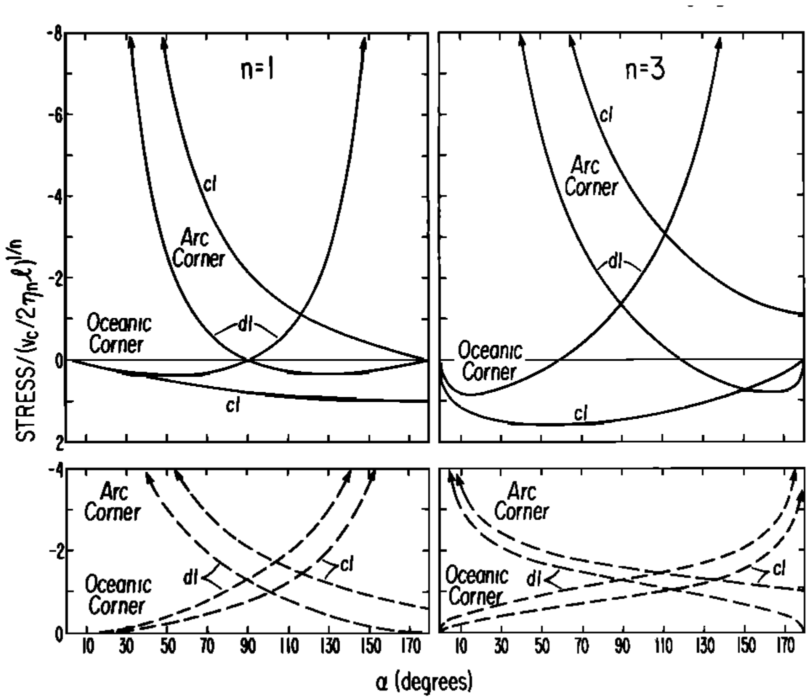

Fig. 4. Pressure (solid curves) and shear stress (dashed curves) on the top (arc corner) and bottom (oceanic corner) surfaces of the descending slab as functions of subduction angle α for (left) Newtonian and (right) non-Newtonian mantles in the coupled lithosphere (cl) model and the decoupled lithosphere (dl) model. Zero degrees corresponds to flat subduction, 90° to vertical subduction, and 180° to overturned subduction.

Tovish et al., JGR, 1978

OK, shows pressure on top ("arc corner") gets very negative [as this happens, presumably load on base of lithosphere above also become very negative--i.e., pulls down]--bottom side not so strong.

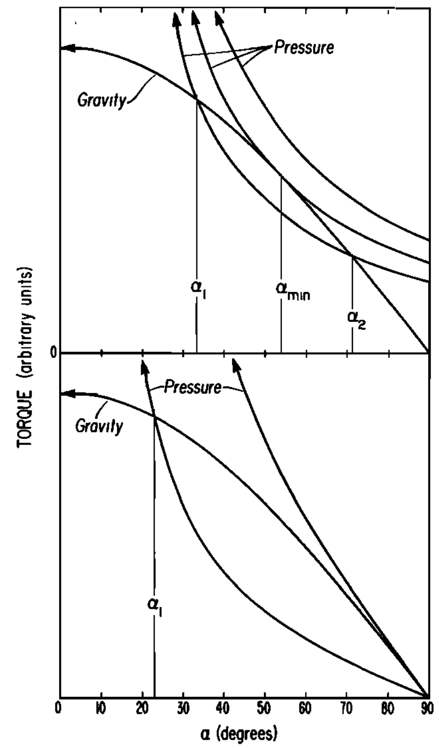

Fig. 6. The absolute values of the torques exerted on the slab by gravity and flow pressures ($n = 3$) as a function of slab dip α. Torques are equal and opposite at angles indicated by the subscripted α's. Several pressure curves are shown to indicate how variations in the relative magnitude of the gravity and pressure torques influence the number and types of equilibrium intersections. (Top) coupled lithosphere model and (bottom) decoupled lithosphere model.

Tovish et al., JGR, 1978

Combining pressure from last slide with weight of slab and then calculating as a torque gives us this--the idea that there is a point where dip is unstable. However, this analysis ignores any deformation within the slab. Although this analysis is basis for Bird's inferences about subsidence, it is not the model preferred by most other mantle-flow modelers.

$$P_{slabtop} = \frac{-8.558\eta U}{r} \text{ for dip=45°}$$

$$P_{slabbottom} = \frac{+0.462\eta U}{r} \text{ for dip=45°}$$

$$P_{upperplate} = \frac{-3.026\eta U}{x} \text{ for dip=45°}$$

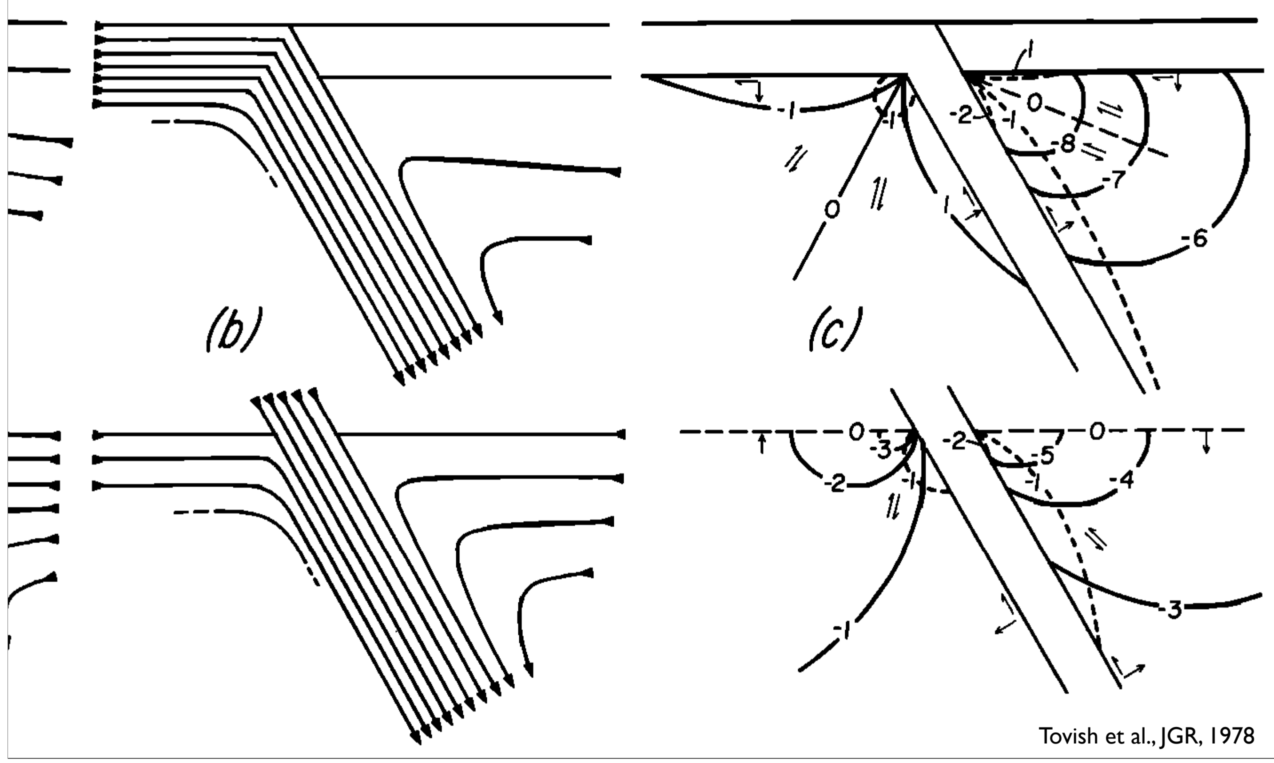

Tovish et al., JGR, 1978

Similarly, we can estimate the force on the upper plate. Math from Turcotte and Schubert section 6.11. So subsidence should vary inversely to distance from the subduction zone. A major complication is that variations in rheology will allow for this to vary a lot.

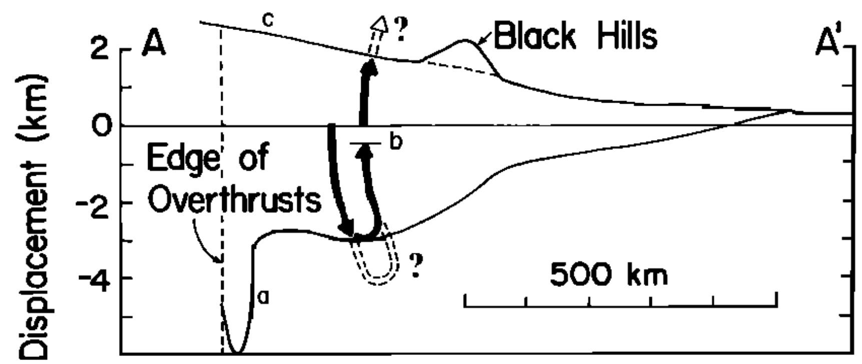

Fig. 5. Approximate estimate of the net effect of Late Cretaceous (including Late Maestrichtian) subsidence and Tertiary uplift for the cross section A-A′ given in Figures 3 and 4. The base of the sequence at the end of its deposition is shown by a. During subsequent uplift to b the surface has uplifted to c. The dashed arrows imply that the solid arrows probably underestimate the total subsidence and uplift.

Mitrovica et al., Tectonics, 1989

Prediction from this model is that if we remove post mid-K seds, things return to flat. Is this true? (certainly not in NE NM, maybe in some places to north).

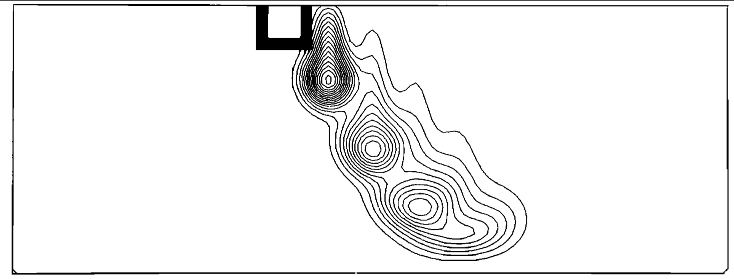

Fig. 10. The thermal field produced by superimposing the $t = 0.0, 0.25, 0.50, 0.75$, and 1.0 fields of the model of Figure 6 ($\Delta t = 0.25$, see text). Each field is horizontally shifted, with respect to the previous field, by an amount equal to the width of the initial block (116 km); only a portion of the cell is shown. The near-surface dip of the resulting subduction is approximately 45°.

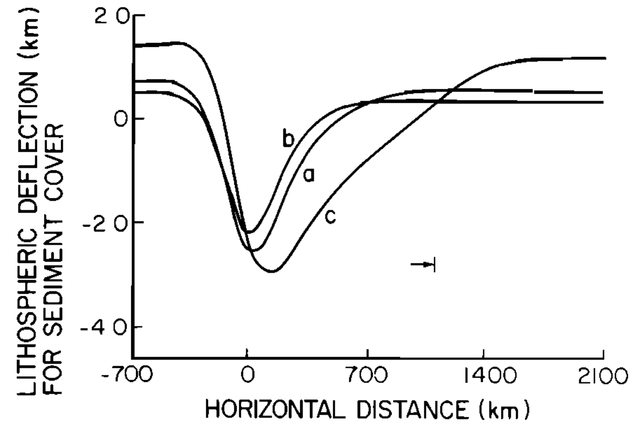

Fig. 11. The topographic profile corresponding to the field of Figure 10 (labeled a). Also shown are the deflections for the cases of near surface dips of 60° ($\Delta t = 0.33$, labeled b) and 30° ($\Delta t = 0.12$, labelled c). In all cases, $D = 5 \times 10^{23}$ Nm. The arrow gives the position of the right boundary of Figure 10.

Mitrovica et al., Tectonics, 1989

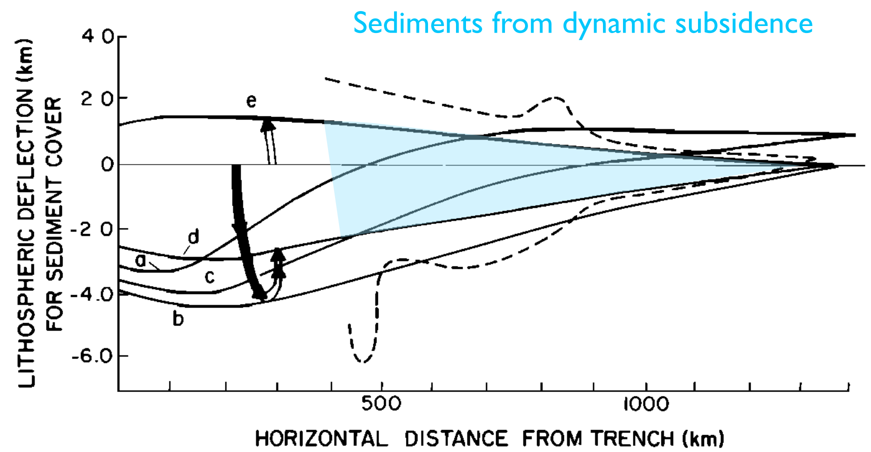

Fig. 16. Profile a, the lithospheric deflection profile corresponding to the subduction zone of Figure 15 except with a dip of 60°. The sequence a, b and c, shows the lithospheric deflection as the subduction geometry moves from 60° dip (a), to 25° dip (b), and back to a 60° dip (c). d gives the deflection 25 m.y. after subduction ceases at the surface. While the basement rebounds from b to d the surface uplifts to e. As in Figure 15, the topographic profiles are computed under the assumption that the sediment cover (of density 2.30×10^3 kg/m^3) remains intact subsequent to the onset of uplift.

Mitrovica et al., Tectonics, 1989

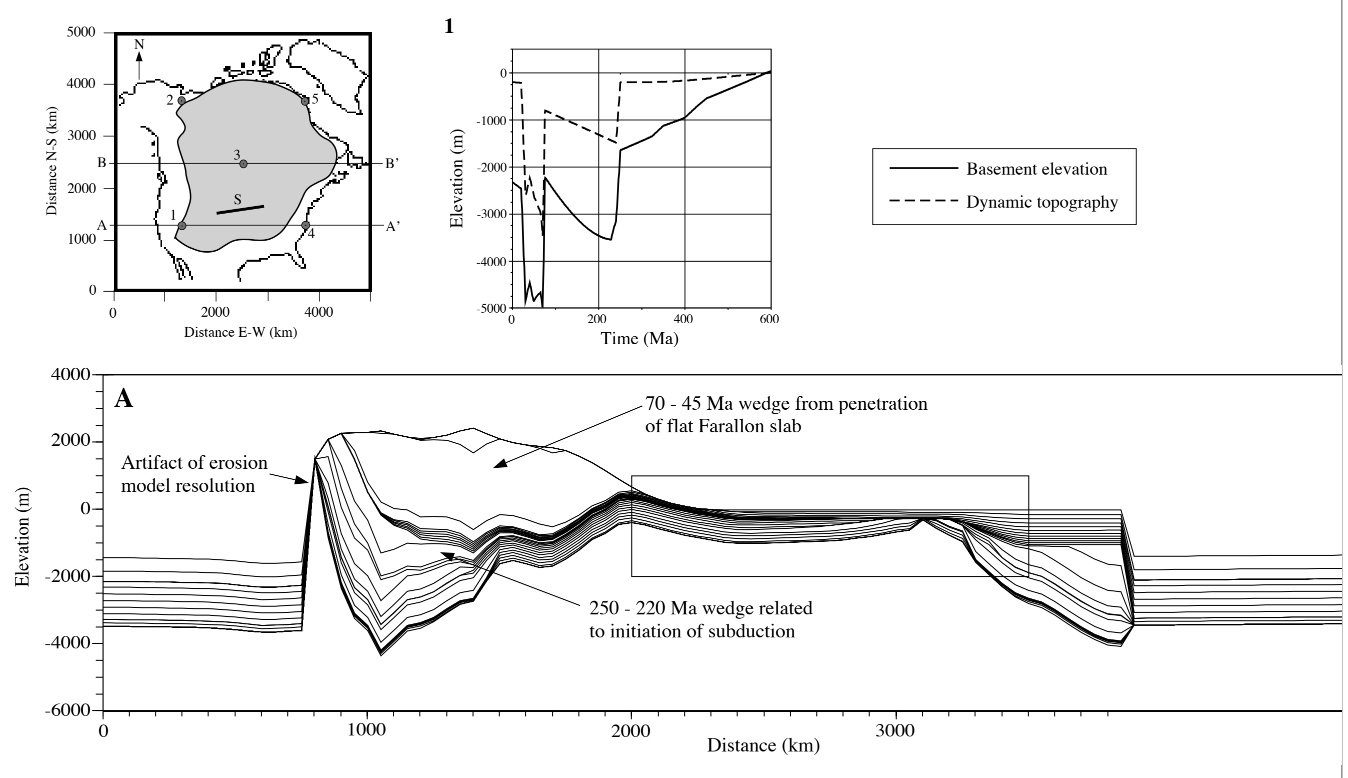

Burgess et al., GSA Bull 1997

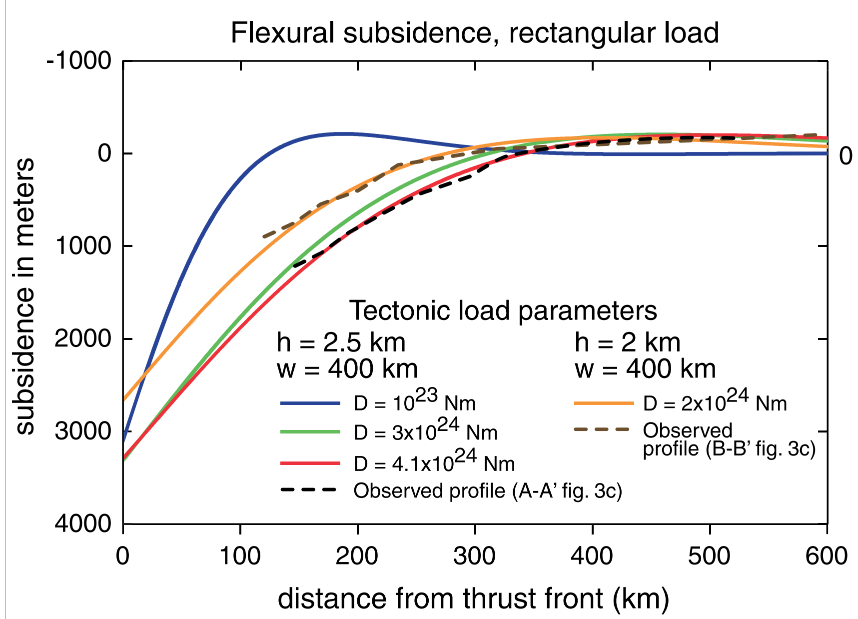

Painter & Carrapa, *GRL* 2013

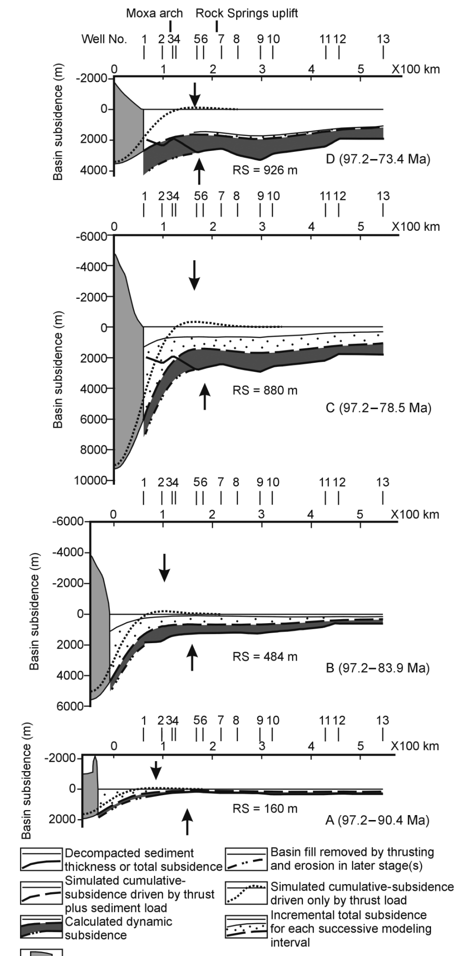

Pang & Nummedal, *Geology* 2004

Pang and Nummedal inferred dynamic subsidence starting c 84 Ma and large by 79 Ma; could also be change in flexural rigidity?

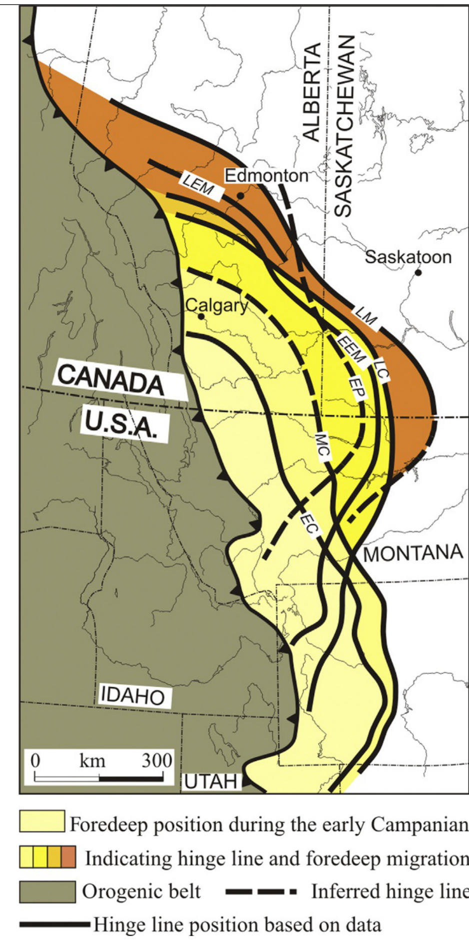

Maill & Catuneanu, in *Sed Basins US & Canada*, 2019,
after Catuneanu et al., *Sed. Geol.,* 2000

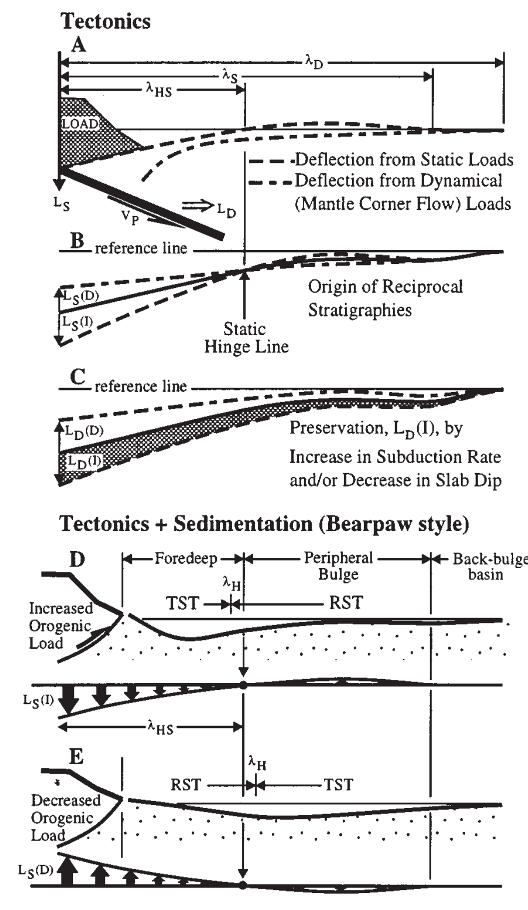

Catuneanu et al., *Geology* 1997

Location of the hingeline between the foredeep and the forebulge during the Campanian–Paleocene. The arcuate trend of the hingeline indicates the locus of greatest flexural load in the orogen—at the center of the arc. Abbreviations: C, M, P, Campanian, Maastrichtian, Paleocene; e, E, Early; l, L, Late. The location of maximum loading shifted progressively northward during the Late Cretaceous–Paleocene (Catuneanu et al., 1999, 2000).

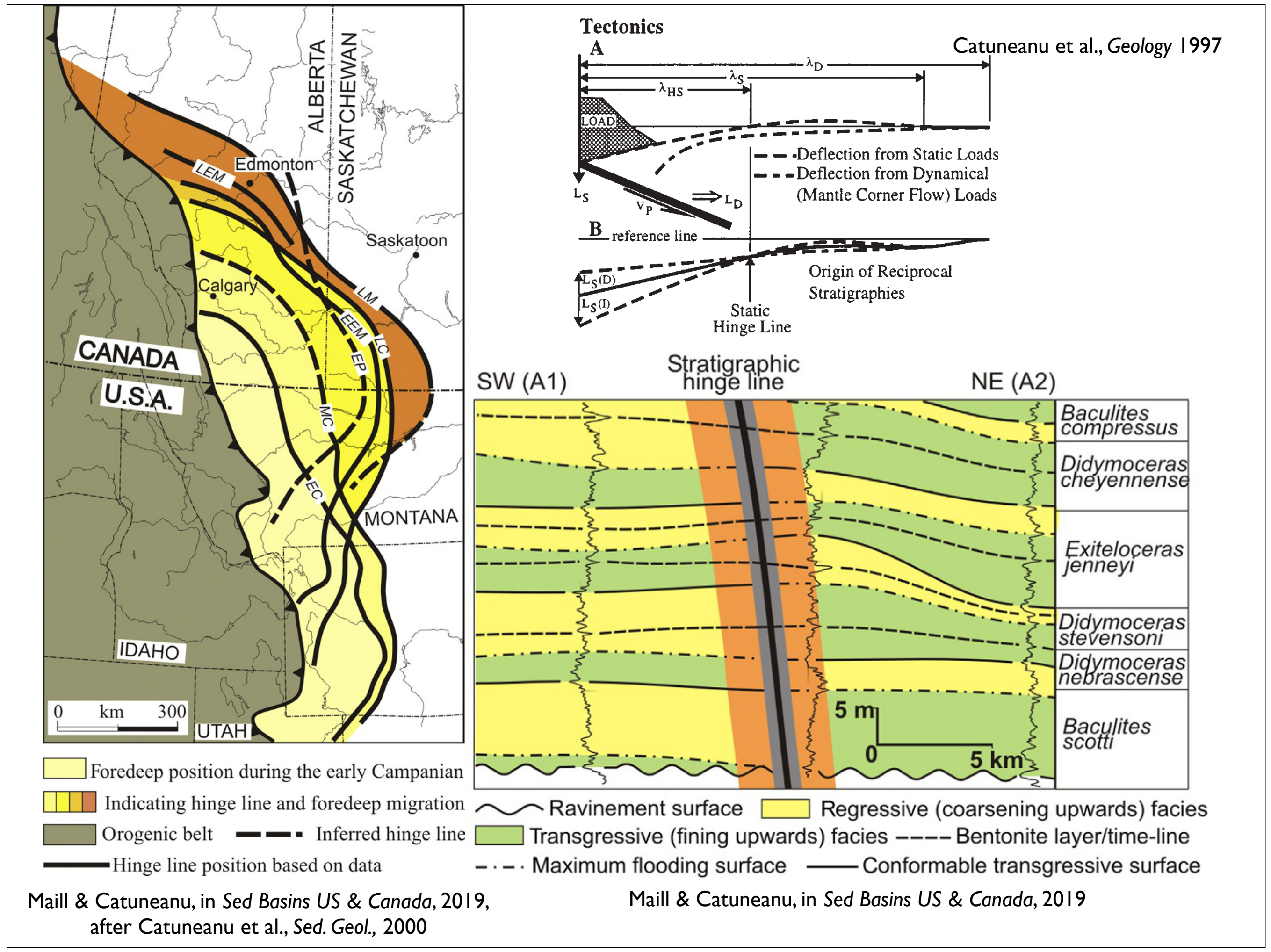

Lower right figure shows reciprocal stratigraphy with biozones and presence of airfall ashes from Alberta.

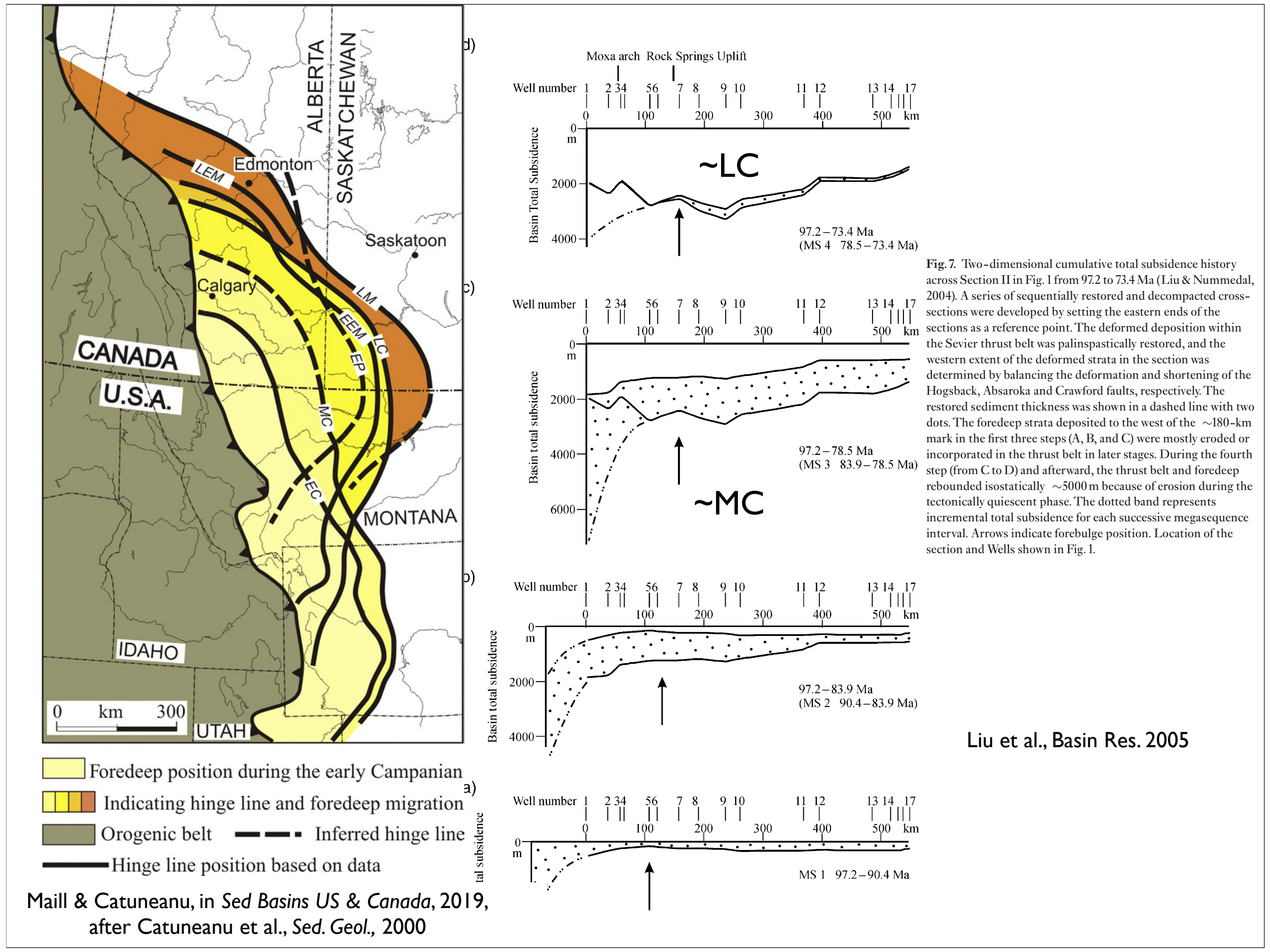

Left is map of hinges inferred by reciprocal strat, right is suggested forebulge position from Liu et al. EC=Early Campanian c. 80 Ma, MC c. 77 Ma, lC c. 73 Ma, EEM = early Early Maastrichtian, c. 71-72 Ma, LEM late Early Maas. c. 70 Ma, LM c. 67-68 Ma, EP = early Paleocene c. 63 Ma

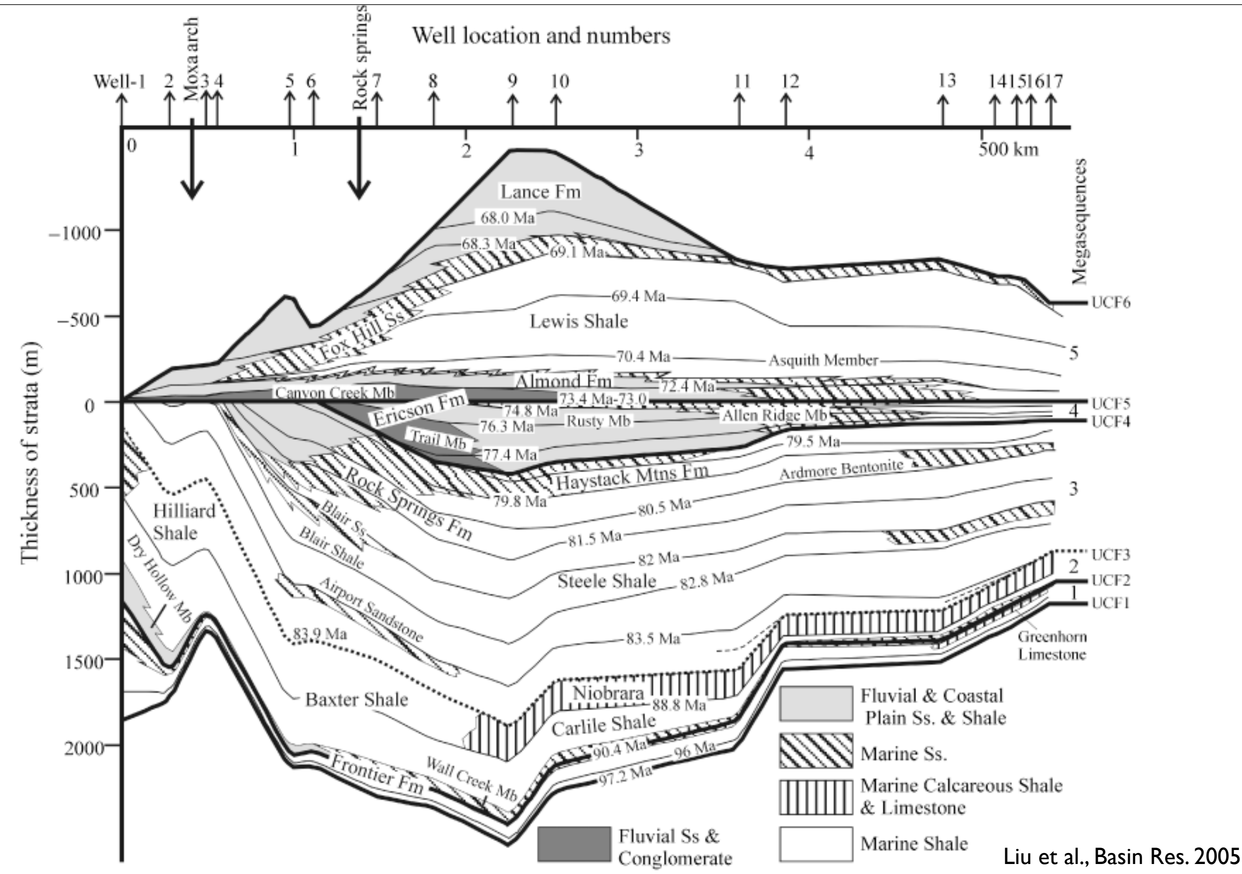

Liu et al., Basin Res. 2005

Fig. 4. Results of well log correlations along cross-section II (Fig. 1), covering the stratigraphic interval from the mid-Cenomanian base of the Frontier Formation to the Maastrichtian Lance Formation (Liu & Nummedal, 2004). Nineteen well logs were correlated. Wells numbers 7 and 10 include two logs sampling different intervals (Wells 7′ and 7″, Wells 10′ and 10″ in Fig. 1) in order to get complete stratigraphic columns. The well log data were collected in Wyoming State Geological Survey. See text for explanation.

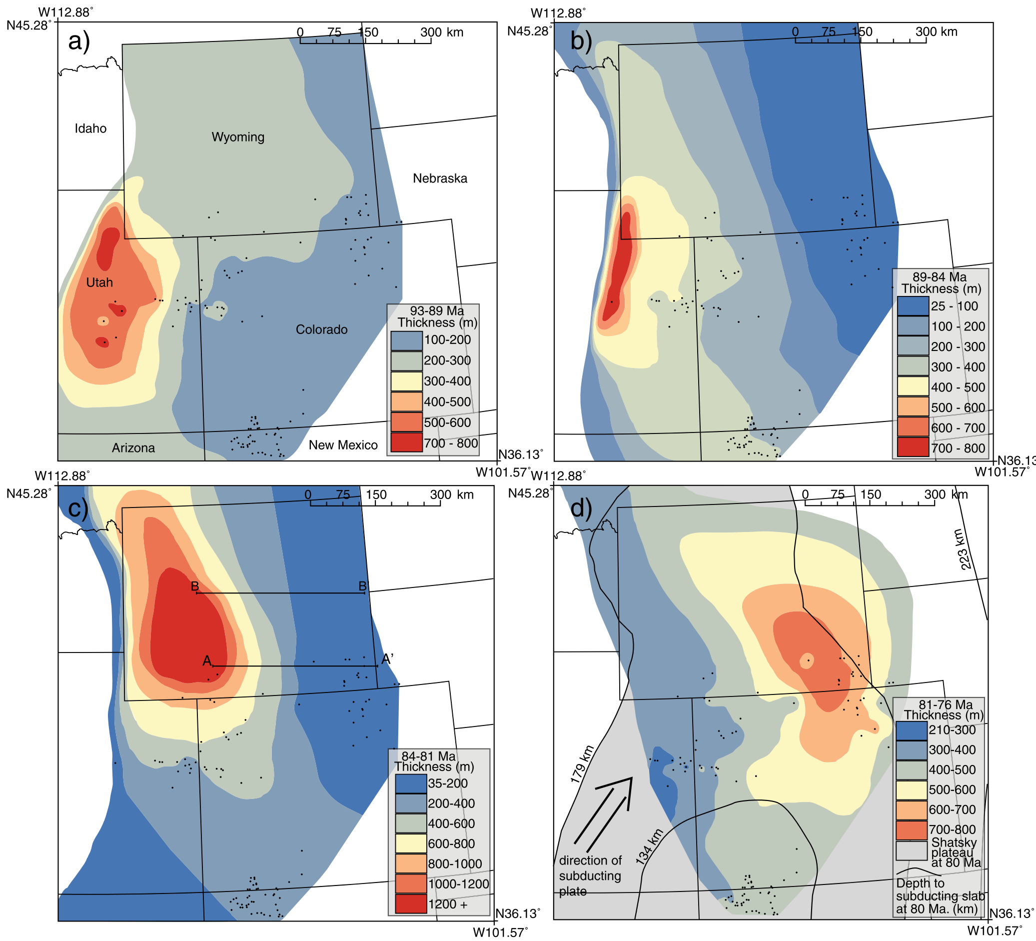

Painter & Carrapa, *GRL* 2013

But will sublithospheric forces that produce a basin also produce stresses consistent with early Laramide deformation?

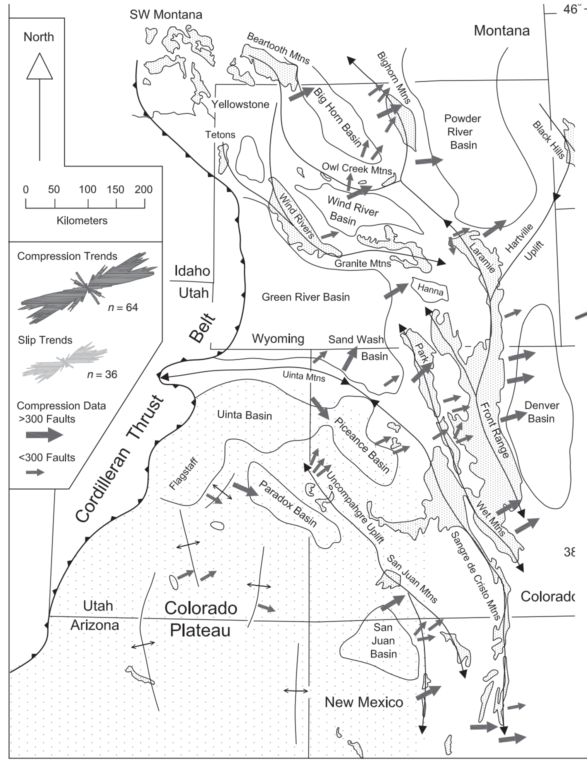

Erslev & Koenig, *GSA Mem 204* 2009

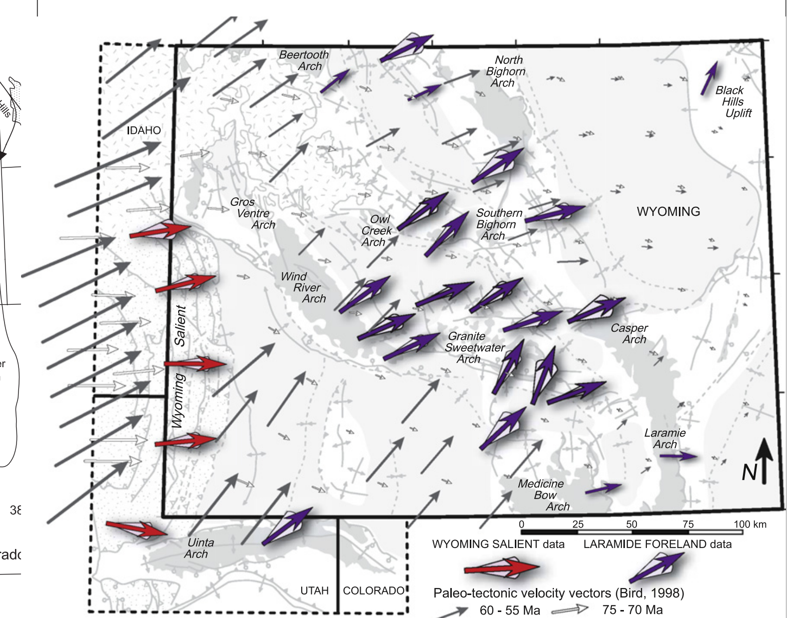

Weil & Yonkee, *EPSL* 2012

Consider loading the lithosphere...

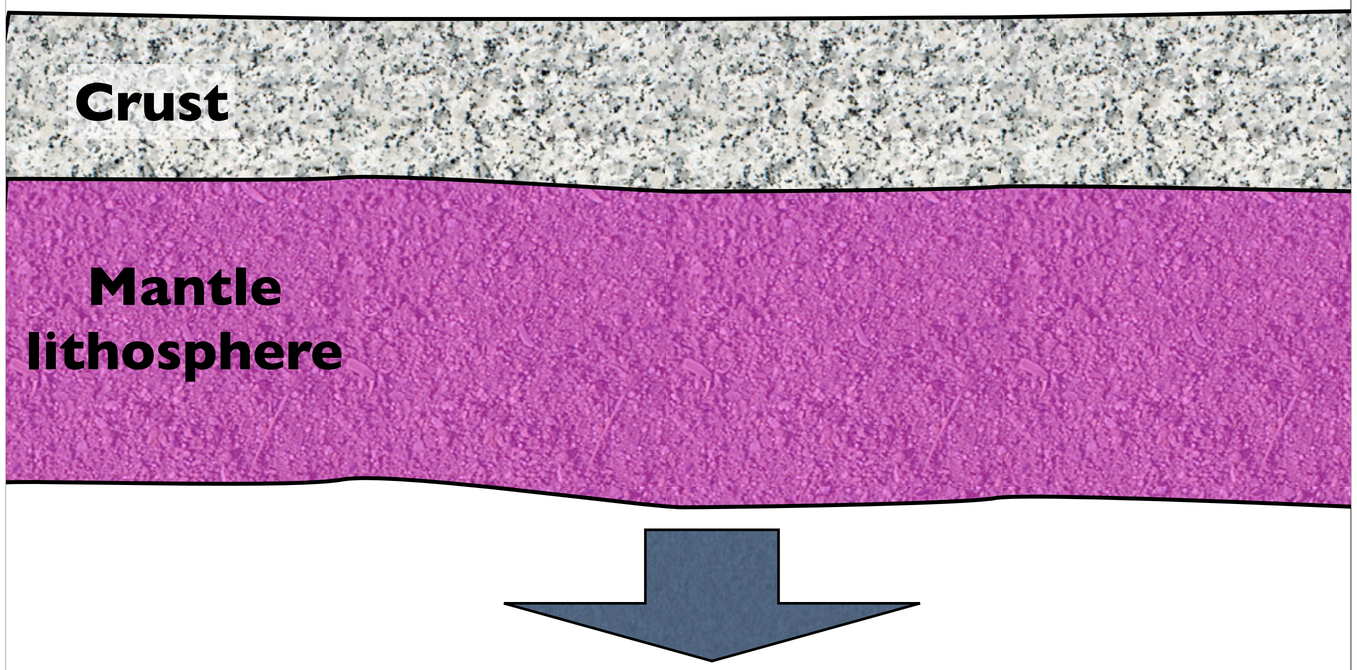

Material is drawn in towards center and area is depressed

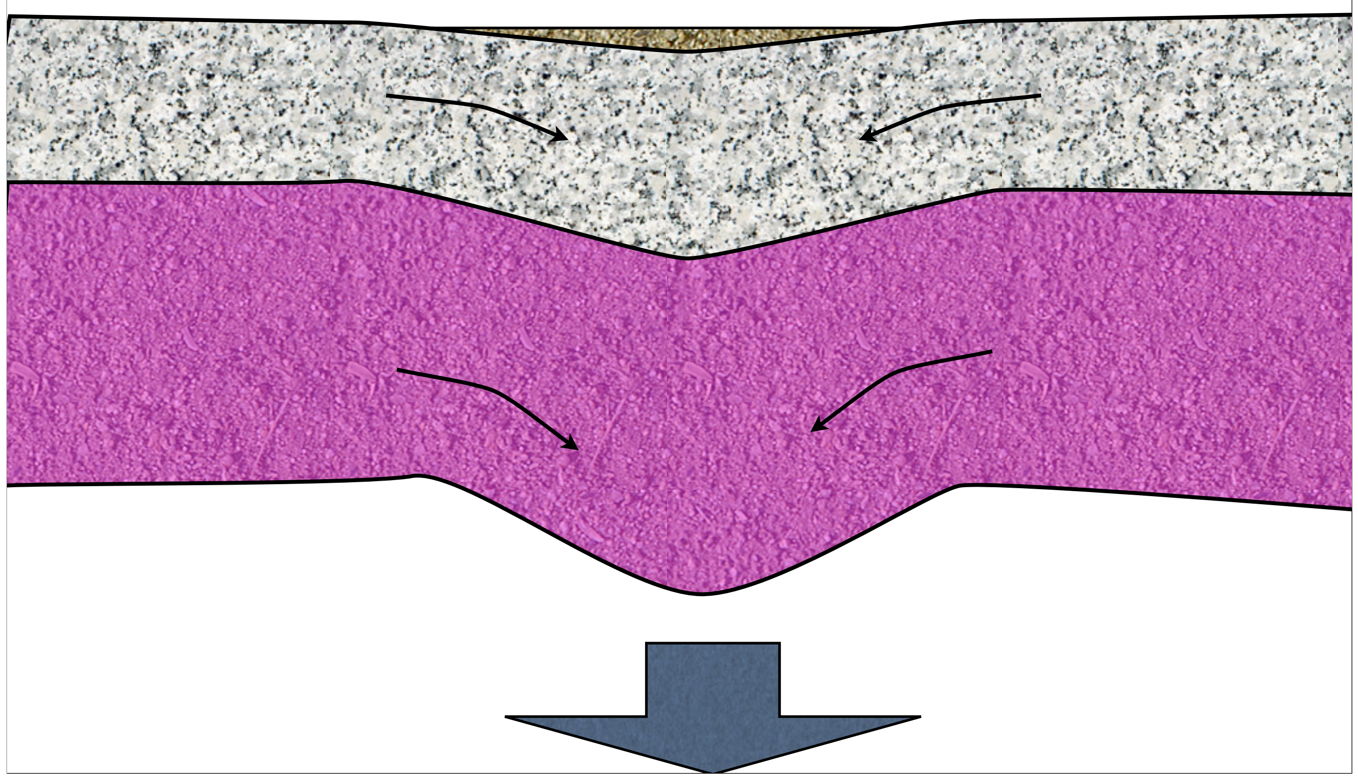

Vertical compressional stresses decrease...
radial compressional stresses increase...
but what of tangential stresses?

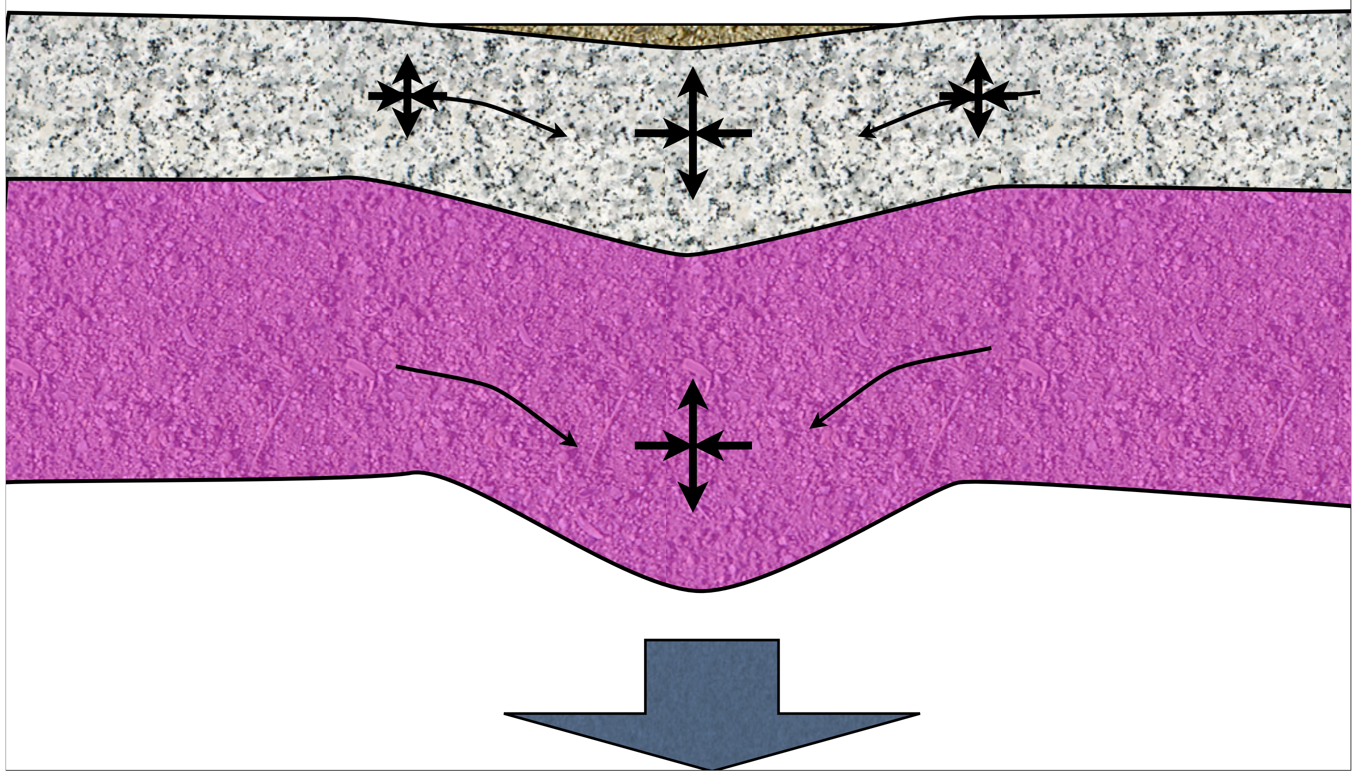

Vertical compressional stresses decrease...
radial compressional stresses increase...
but what of tangential stresses?

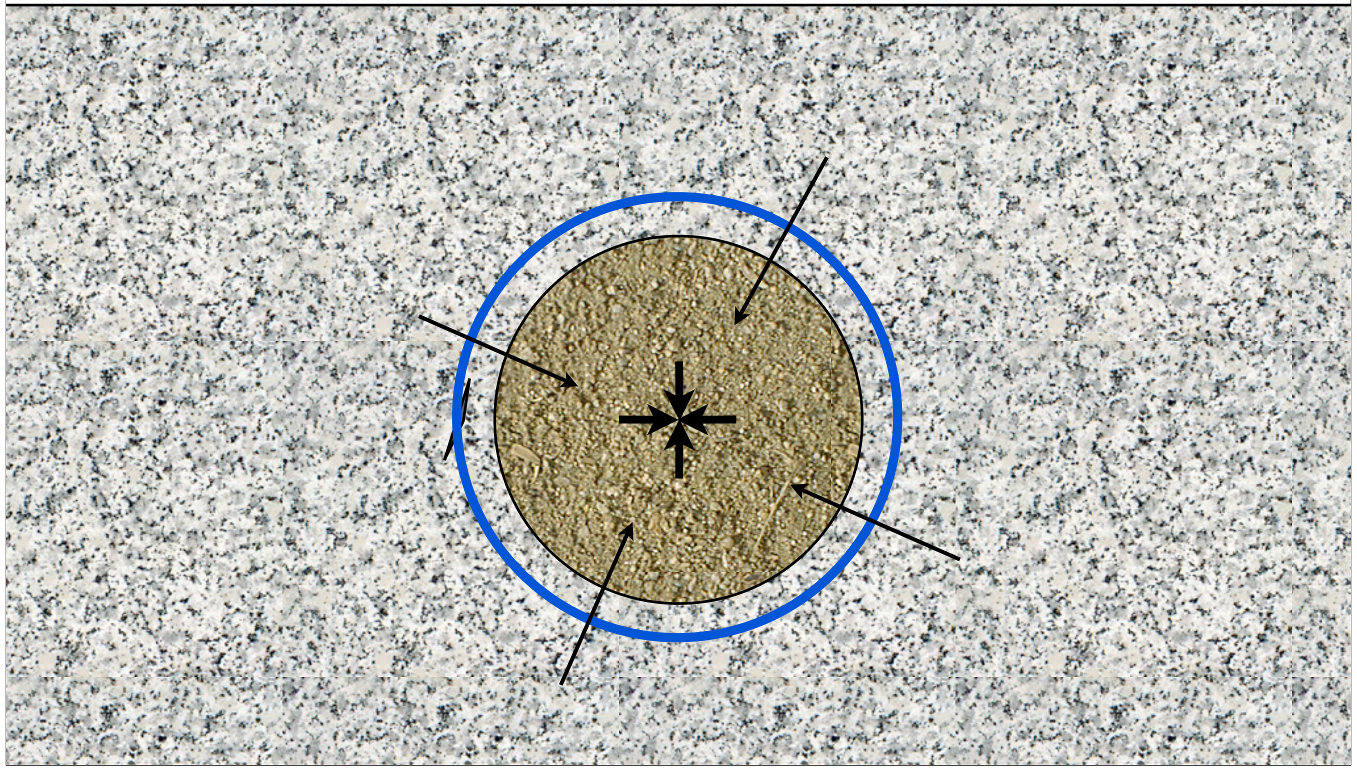

As material moves in, hoop stresses get strongly compressional

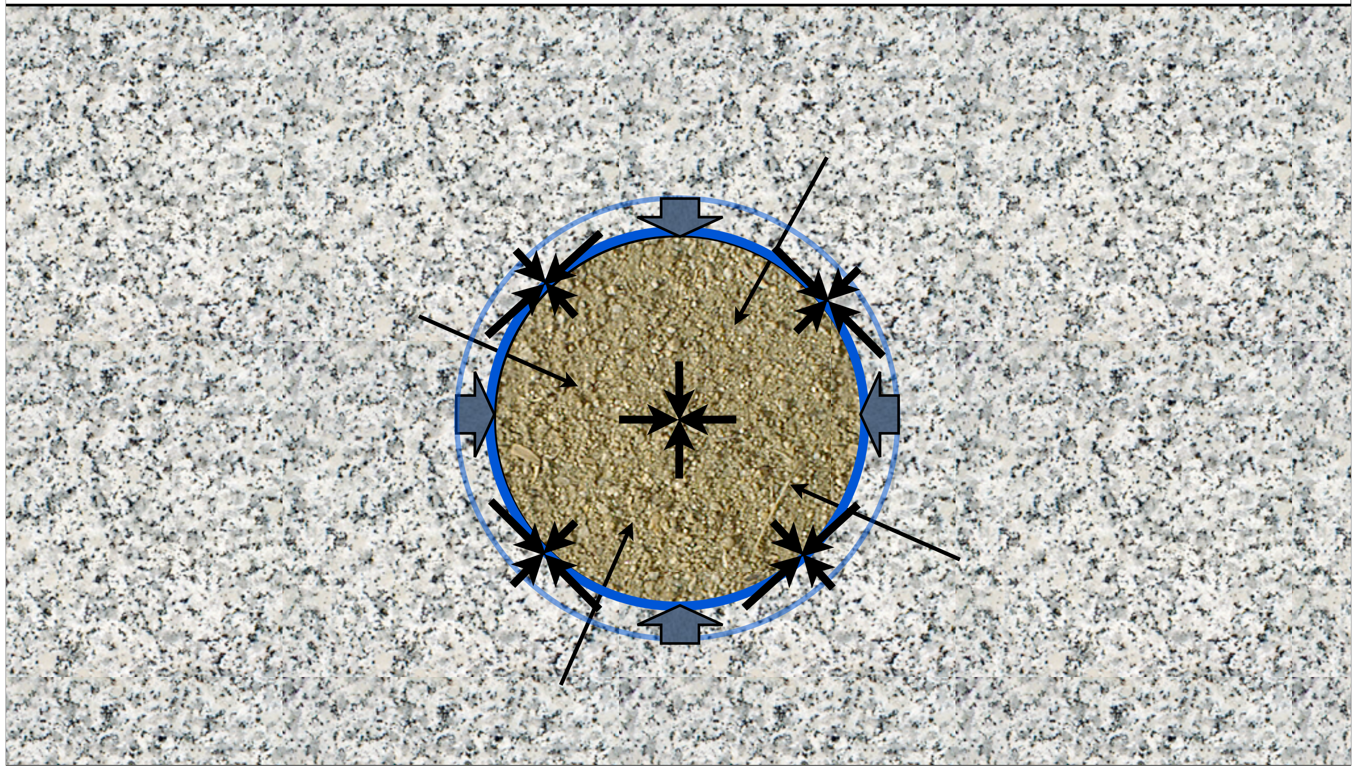

So you could expect radially symmetric folding or faulting
But what if there is a regional stress field?

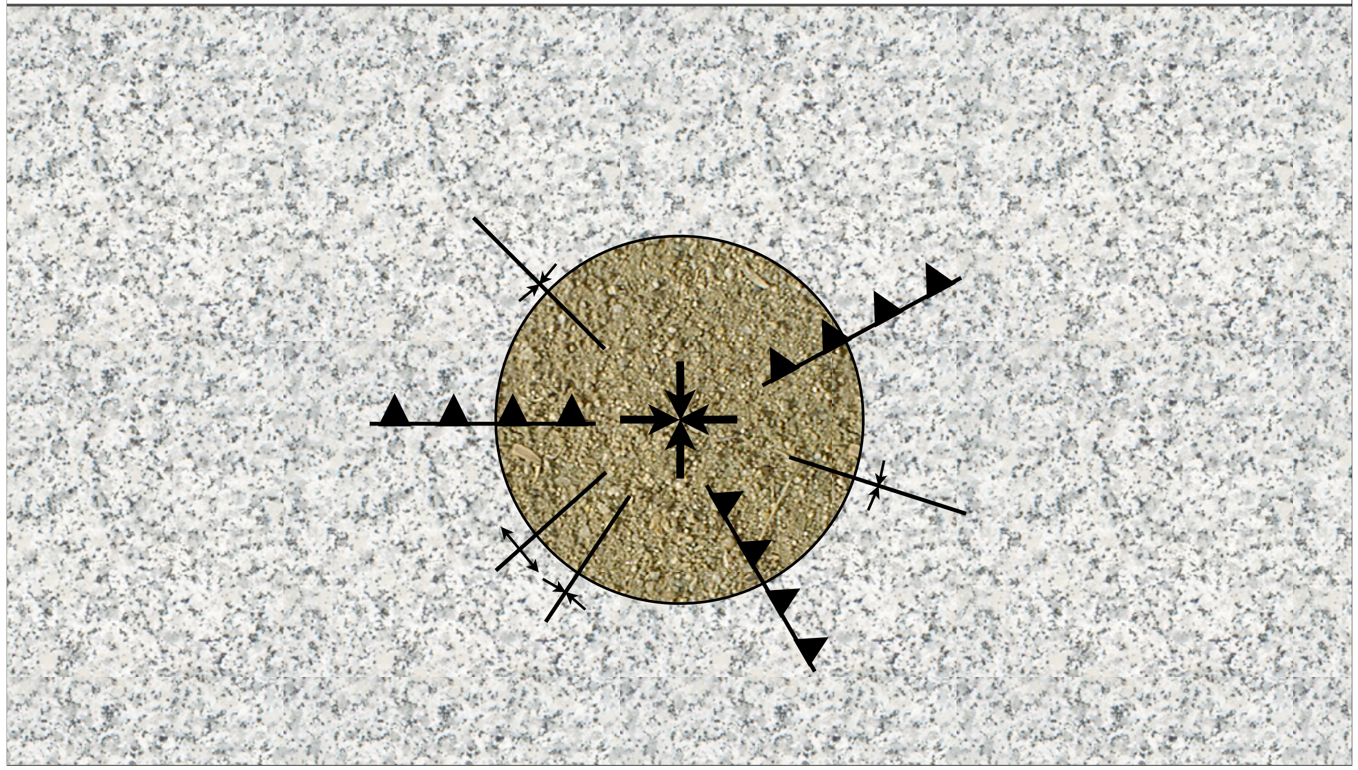

Estimate overall stress field:

Uniform east-west compression

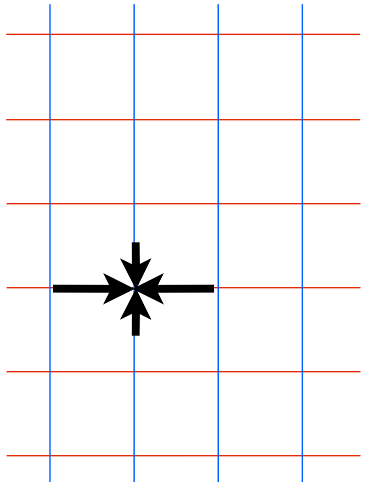

+

Stresses above a sinking sphere (Morgan, 1965)

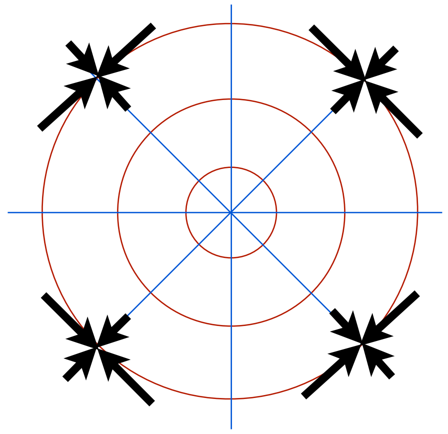

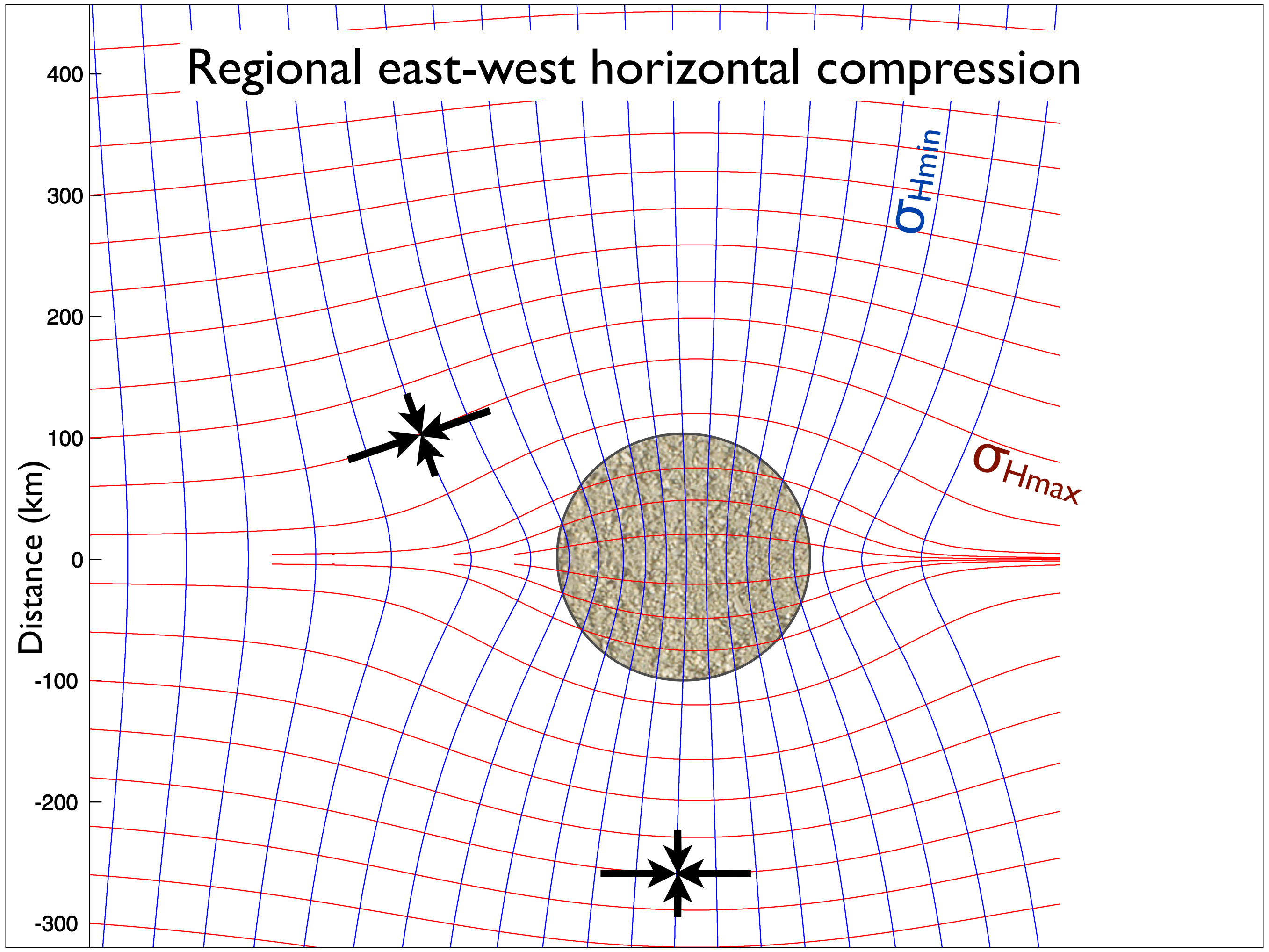

Exact degree of bending of stresses depends on the ratio of the load to the regional stress field.

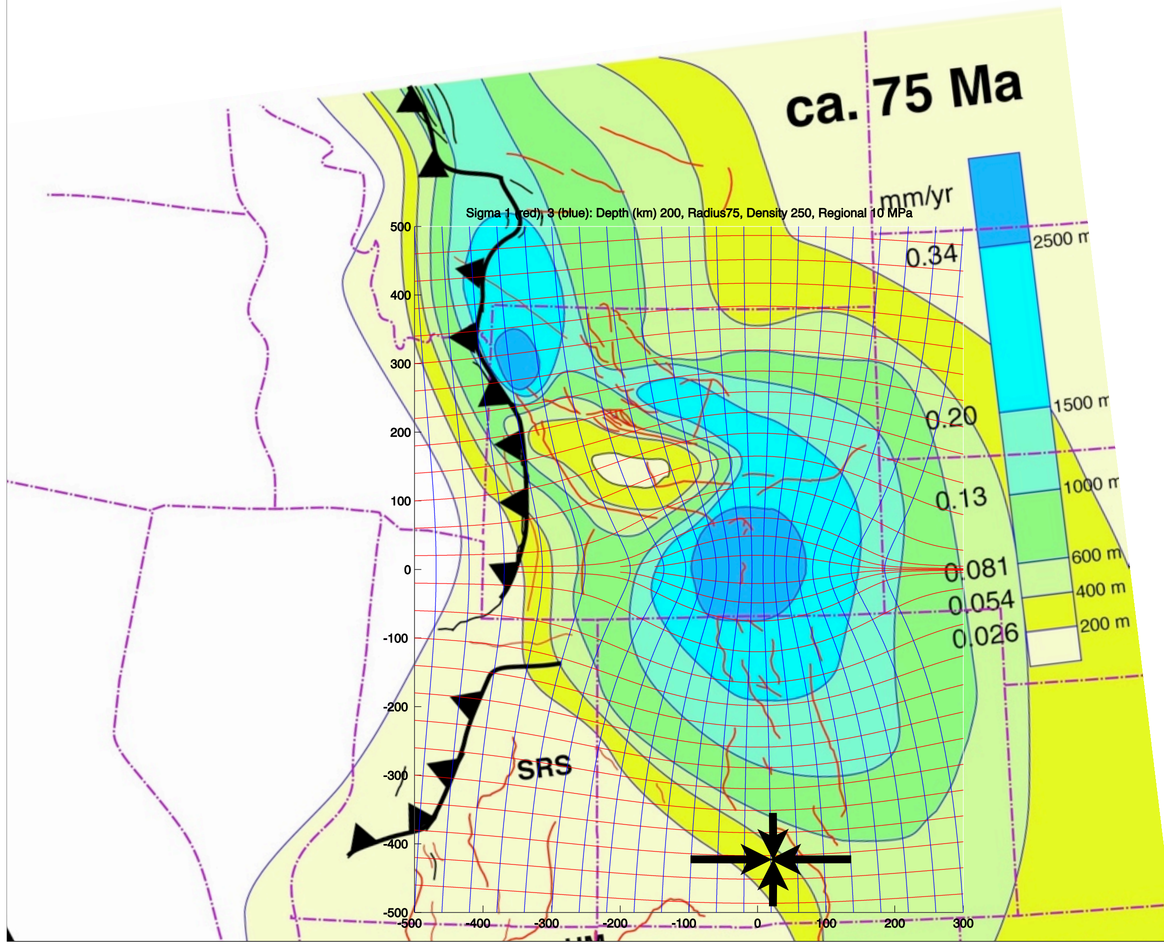

ca. 75 Ma
mm/yr
Sigma 1 (red), 3 (blue): Depth (km) 200, Radius75, Density 250, Regional 10 MPa
0.34
0.20
0.13
0.081
0.054
0.026
2500 m
1500 m
1000 m
600 m
400 m
200 m
SRS
500
400
300
200
100
0
-100
-200
-300
-400
-500
-500
-400
-300
-200
-100
0
100
200
300

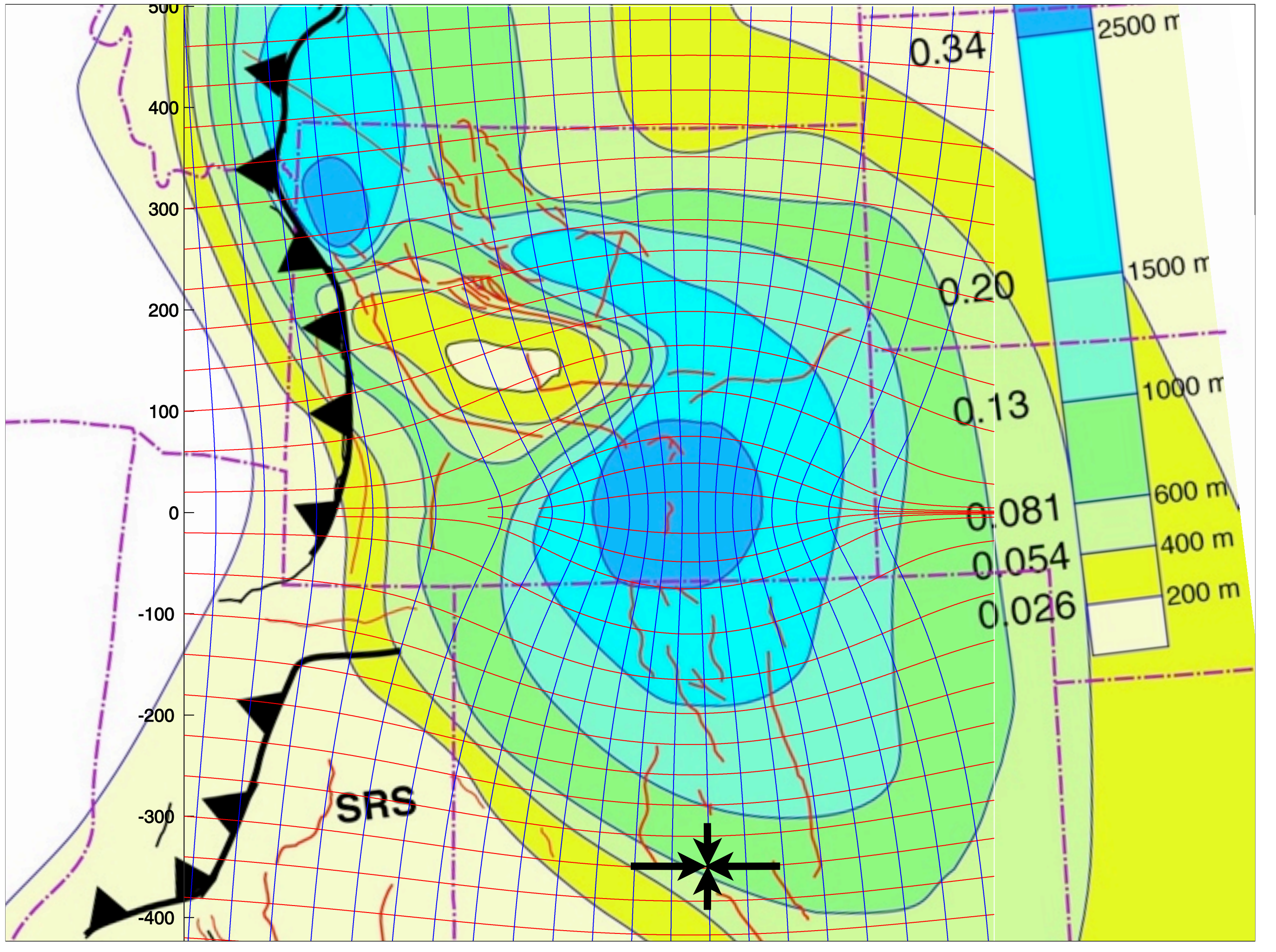

500
400
300
200
100
0
-100
-200
-300
-400
SRS
0.34
0.20
0.13
0.081
0.054
0.026
2500 m
1500 m
1000 m
600 m
400 m
200 m

Uplifts mostly normal to σ_{Hmax}

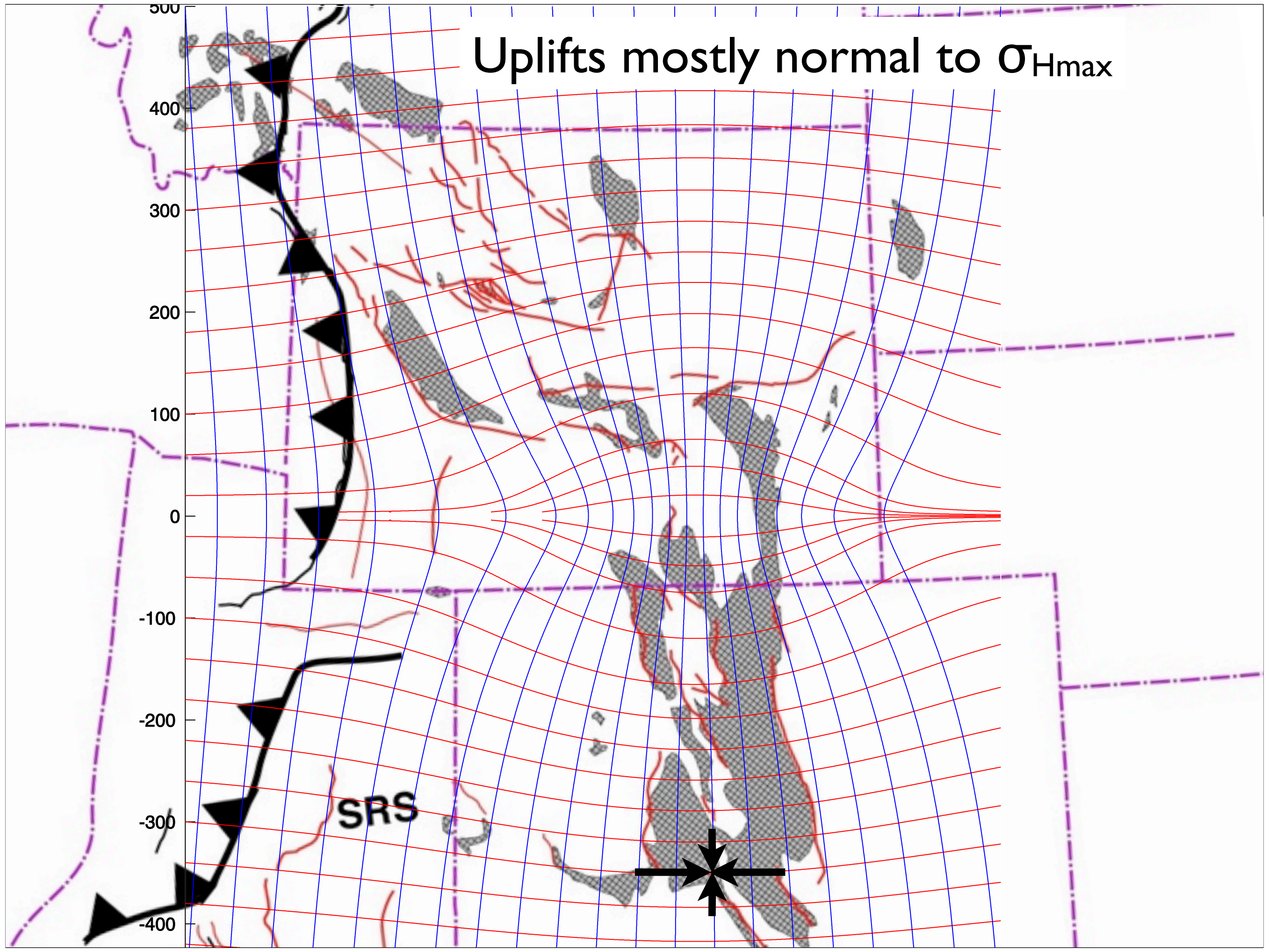

Inferred stresses even closer to those measured

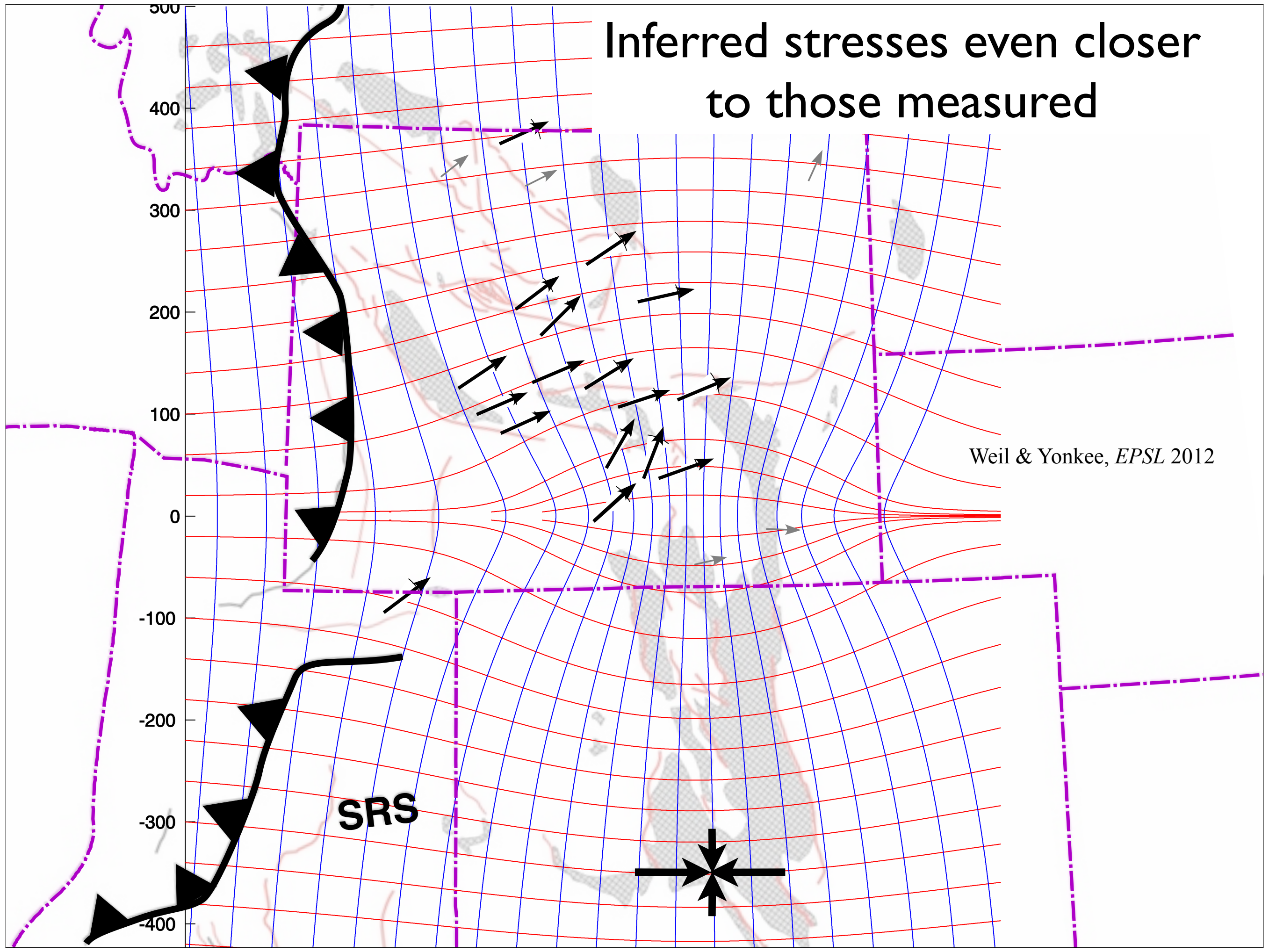

Inferred stresses even closer to those measured

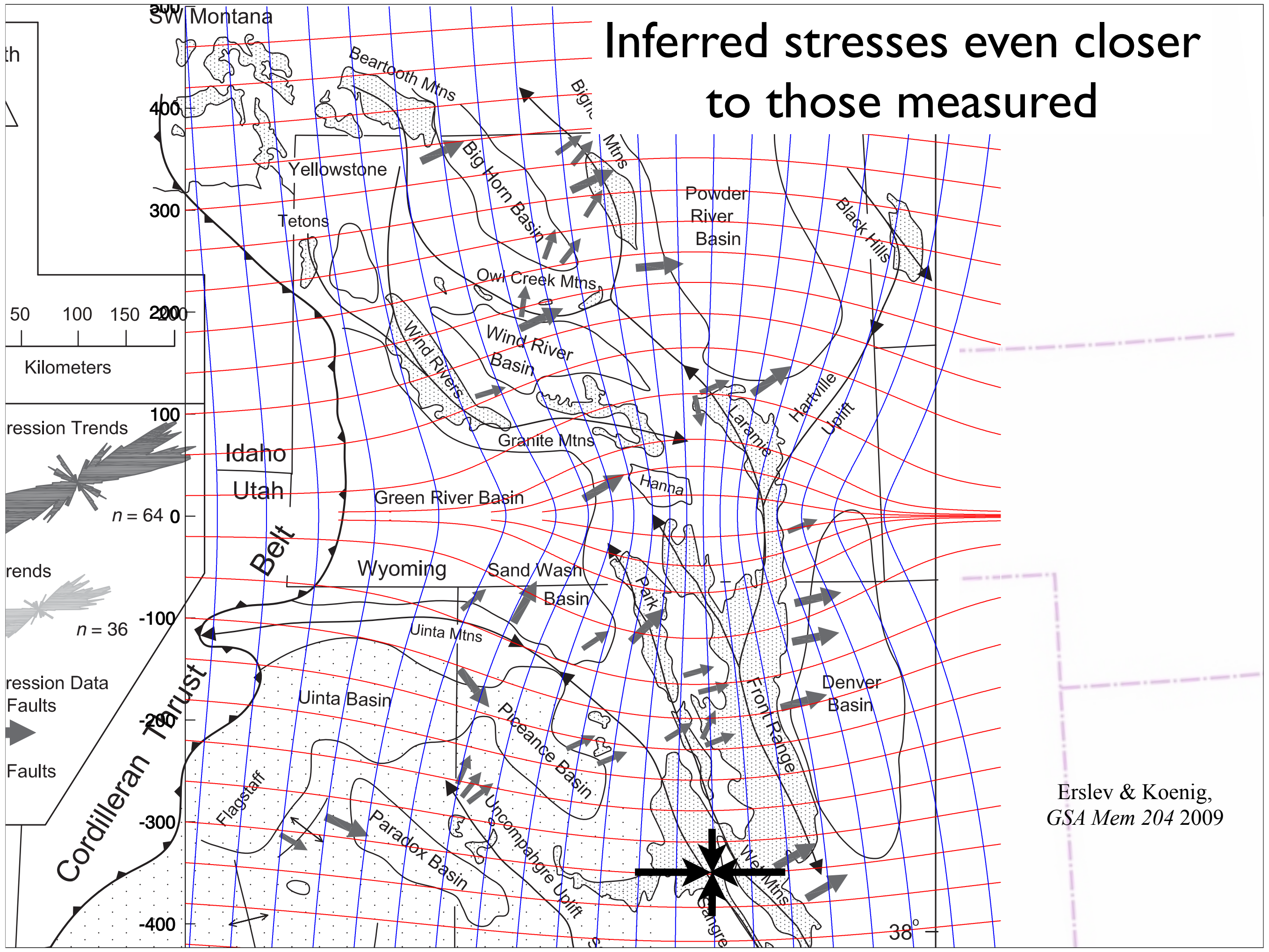

Erslev & Koenig, *GSA Mem 204* 2009